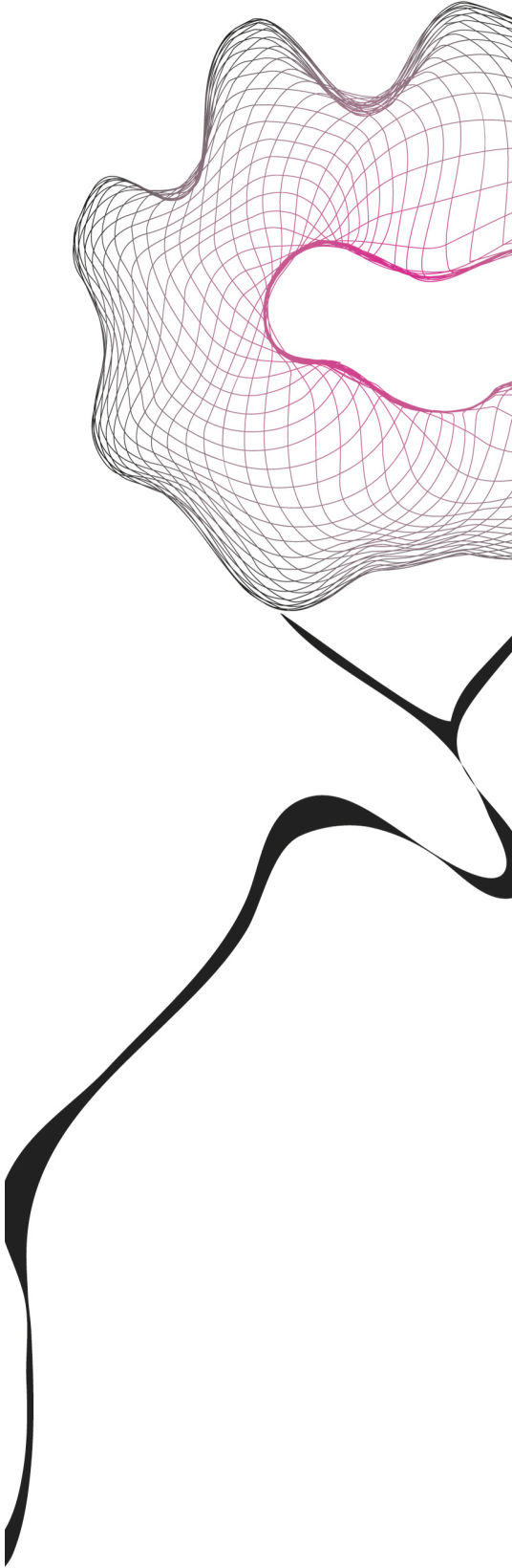


MASTER THESIS



DETECTION OF
INTERICTAL
EPILEPTIFORM
DISCHARGES IN EEG

A.J.E. Geerts

APPLIED MATHEMATICS
HYBRID SYSTEMS

EXAMINATION COMMITTEE

dr. ir. G. Meinsma
prof. dr. ir. M.J.A.M. van Putten
S.S. Lodder
prof. dr. A.A. Stoorvogel
dr. H.G.E. Meijer

DOCUMENT NUMBER
M2012 - 17314

Detection of Interictal Epileptiform Discharges in EEG

Master Thesis in Applied Mathematics
by
A.J.E. Geerts

September 18, 2012

Supervisors:

dr. ir. G. Meinsma (daily)
prof. dr. ir. M.J.A.M. van Putten
S.S. Lodder

UNIVERSITY OF TWENTE.

Faculty of Electrical Engineering, Mathematics and Computer Science
Department of Applied Mathematics
E-mail: info@ewi.utwente.nl

The diagnosis of epilepsy heavily depends on the detection of *epileptiform discharges* in interictal EEG, the EEG in between two seizures. By visual analysis a physician wants to detect these epileptiform discharges (*spikes*). Due to the wide variety of morphologies of epileptiform discharges, and their similarity to waves that are part of normal EEG or to artifacts, this detection is far from straightforward. Moreover, it is a time consuming task, holding back for the analysis of long-term recordings, which would improve the detection of evidence of epilepsy [17, 18].

In this study a first step has been made towards automated detection. We would like to find events with a heightened chance of being an epileptiform discharge. All other parts of the EEG can then be neglected, resulting in a reduction of the time needed to analyse a record.

In this study we investigated two methods: wavelet analysis and matched filtering. The choice for *wavelet analysis* was motivated from literature. A big drawback of wavelet analysis turns out to be the limited choice for templates with which to correlate the signal. Therefore we propose to use *matched filtering* in which we are not restricted in the choice for templates. Classically, mathed filtering considers an event (spike) ‘detected’ if some correlation exceeds a certain threshold. We added a power threshold, claiming that the template has to explain for a certain percentage of the signal power before an event is considered to be of an epileptiform kind. This resulted in a *sensitivity* (percentage of true spikes that are detected) of 86.41% with 0.1503 *False Positives per Minute (FPM)* if this threshold was set to 75%. This is showed to be a lower bound for the data set, consisting of 10 EEG recordings, as we were able to obtain a sensitivity of 95.63% with an FPM of 0.2002 as well for slightly different threshold settings.

This approach is not suitable for automation. It requires the selection of a suitable template before matched filtering can be applied, implying that the entire recording needs to be scanned first. It, however, shows the strength of matched filtering and the present with a library of spikes is therefore proposed for the goal of automated

spike detection. Preliminary results, with a library of just 9 templates and a fairly simple rules defining an event as epileptiform or not, show this to be promising as we already reach sensitivities of around 80% with few false positives per minute.

My parents often use the phrase

”Time flies when having fun!”

It is exactly that what pops into mind when I am writing this preface, knowing that six years of study have almost come to an end. Six years that feel to have flown by. It feels like only yesterday (well okay, maybe not yesterday, but you know what I mean) that I came to Enschede, where I felt at home right away. Looking back, these six years have brought me a lot. Not only did I find the desired challenge in the study, being part of the board of W.S.G. Abacus and working on several jobs for the department Applied Mathematics, I got the opportunity to develop myself even more. Being a student in Enschede I also got the chance to discover triathlon and knotsbal, to fall in love with Twente and make a lot of friends.

This is not to say that it was easy to reach this point. I had to work hard and have had some difficult times, really not knowing why I ever wanted to be an applied mathematician. It did not come easy, but I persisted though. This makes me proud to be where I am now, on the verge of being an applied mathematician, looking back with a smile on my face.

Astrid Geerts
September 2012

Contents

Abstract	iii
Preface	v
Contents	vii
1 Introduction	1
1.1 Motivation	1
1.2 Related Work	3
1.3 Research Goal	4
1.4 Structure of the Report	4
2 Theoretical Framework	5
2.1 Electroencephalography	5
2.2 Interictal Epileptiform Discharges	7
2.3 Performance Measures	10
2.4 Preprocessing	12
3 Wavelet Analysis	15
3.1 An introduction to wavelet analysis	15
3.2 Continuous-time wavelet transform	20
3.3 Applications of wavelet analysis	20
3.4 Wavelet analysis in spike detection	23
3.5 Summary	26
4 Matched Filtering	27
4.1 Theory of Matched Filtering	27
4.2 Ratio of Powers	30
4.3 Academic Example	31

4.4 Summary	33
5 Matched Filtering in Practice	35
5.1 Implementation	35
5.2 Results	37
5.3 Library of Templates	40
6 Conclusion	41
7 Discussion and Recommendations	43
Appendices	47
A Templates	47
B Matlab Scripts	51
Bibliography	57

CHAPTER 1

Introduction

This chapter introduces the reader to the world of automatic spike detection in electroencephalography. It will become clear what a spike is, why we want to detect it (Section 1.1) and what already has been done to automate this detection (Section 1.2). In Section 1.3 the research goal of this master thesis regarding automatic spike detection is formulated. Finally, Section 1.4 gives an overview of the structure of the report.

1.1 Motivation

Epilepsy is a neurological disorder characterized by recurrent and unprovoked *seizures*. The effects of seizures differ, ranging from absences (episodes of unresponsive staring) up to uncontrolled muscle contractions throughout the entire body (probably best known by the broad audience).

Epileptic seizures are the result of occasional, sudden and excessive electrical discharge of the brain gray matter [12]. *Electroencephalography (EEG)*, a clinical tool that measures the electrical activity along the scalp, will clearly show this abnormal, synchronized and excessive electrical activity in the brain as is clarified by Figure 1.1.

Seizures are unprovoked and months, or even years, can pass without a seizure occurring. Therefore it is not practical (and unethical) to monitor a patient on EEG and wait for a seizure to occur. However, *interictal EEG*, the EEG in between seizures, of a patient with epilepsy is characterized by occasional *epileptiform discharges*. The detection of these discharges (also referred to as *spikes*) is leading in the diagnosis of epilepsy, diagnosis which is important to give a patient adequate medical support.

Electroencephalographers are to determine the presence of these spikes by visual analysis. This is not only a task that requires expertise, it is also time-consuming,

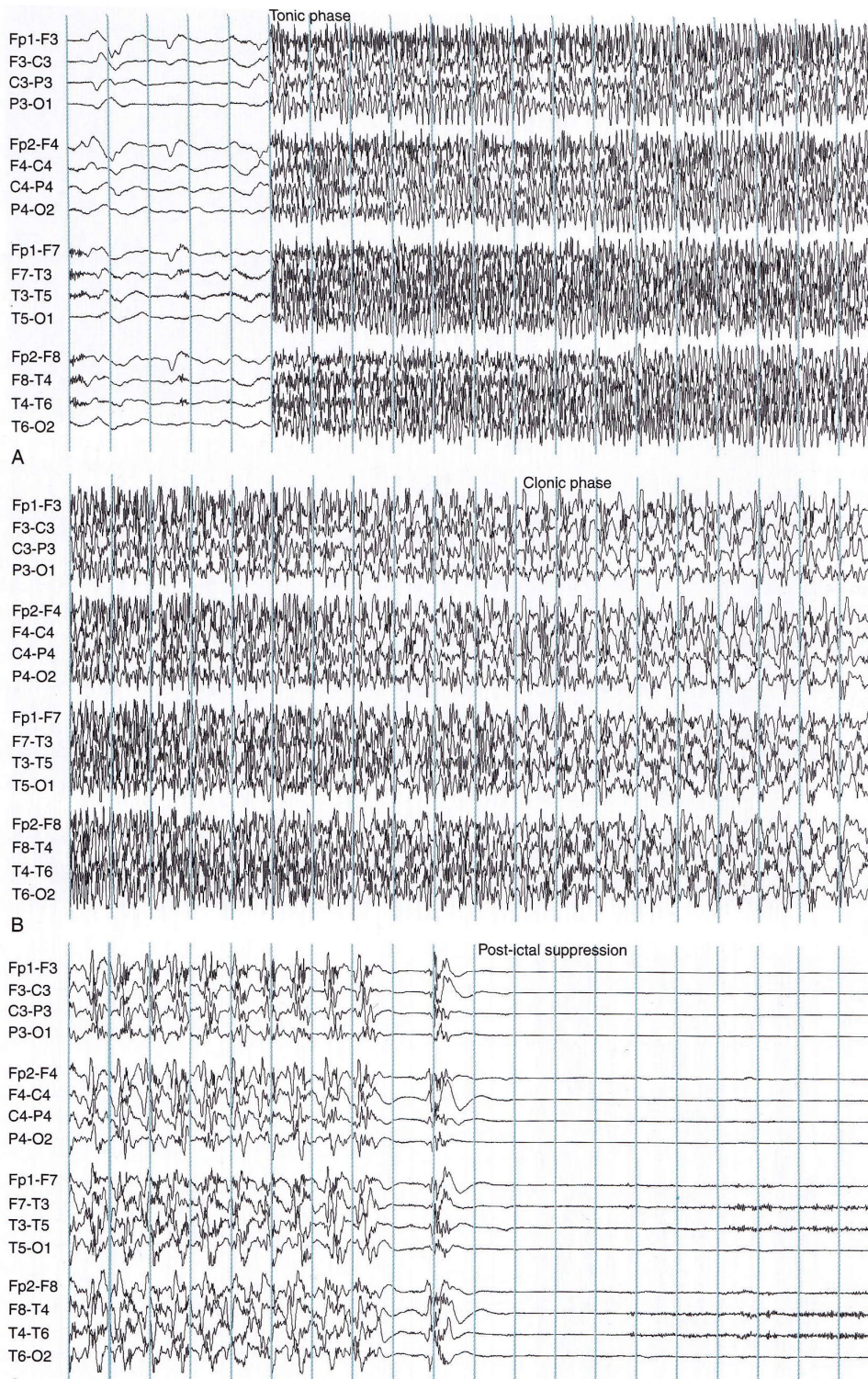


Figure 1.1: *The classical evolution of a generalized seizure. There is abrupt onset of generalized rapid spikes and we see post-ictal suppression when seizure discharges come to an halt [15].*

especially in the case of long-term recordings. Therefore, automatic assistance, which will reduce the analysing time, is desirable.

Automated interpretation software has been developed to offer this desired assistance. Due to high numbers of false detection, however, they are hardly used in practice [1, 10]. A complicating factor is that it is not unusual for two readers of the same record to disagree on the nature of observed features [10]. Difficulties arise due to the wide variety of morphologies of epileptiform discharges, and their similarity to waves that are part of normal EEG (such as the vertex waves and K-complexes during sleep) or to artifacts such as eyeblinks. This makes the detection of epileptiform discharges far from straightforward.

1.2 Related Work

Automatic detection of *interictal epileptiform discharges (IEDs)* has been a research goal since more than forty years. Many methods have been developed in these years, but none of them proved to be as reliable as an experienced EEG-reader [10].

The methods can be classified by their mathematical approach. At first, *mimetic analysis* will be discussed. Such an approach analyses the signal waveform in a way similar to how humans would describe it. The morphological description used in this approach turned out to be insufficient though, because many transients, normal, abnormal or artifactual, fit the same definition.

In *template matching*, a spike is found when the cross-correlation between a chosen template and the EEG record exceeds a certain threshold. This approach was mainly used in the early years of research [6, 24] and it struggled with the same problem as mimetic analysis.

The assumption that the background EEG is stationary, i.e. mean, variance, and autocorrelation function do not change over time, forms the basis for *parametric methods*. In such an approach, an IED is detected if the recorded behaviour differs from the behaviour predicted by the model parameters. This method did not work well, because IEDs turned out to be more stationary than expected.

Power spectral analysis describes how the power of a signal is distributed over its frequency. If the frequency band corresponding to spikes is dominant, an epileptiform event is considered. Several transforms have been used to transform the signal from the time domain to the frequency domain, among which the Fourier, Hilbert and Walsh transforms. A drawback of these methods is their fixed time-frequency resolution.

Wavelet analysis is an advanced matching technique. By scaling and translating a mother wavelet (template) the fixed time-frequency resolution problems of power spectral analysis can be overcome. Wavelet analysis comes with the price of a limited choice for templates.

Finally, we have *artificial neural networks* that consist of ‘artificial neurons’, the basic units of the network that can be trained to recognize patterns in ways similar to humans [10]. Artificial neural networks need no specific rules, but are trained by

examples. By providing the system classified examples of both spike and non-spike events it can be trained in the recognition of IEDs.

1.2.1 Remarks

Two remarks about comparing the performance of different algorithms have to be made. The first is that the comparison is difficult because each study uses its own EEG dataset [10]. Secondly, the inter-reader sensitivity in a study with five expert EEG readers was found to be 0.79 [27], i.e. there is no golden standard that can be used in the evaluation of the performance of algorithms. To overcome the first problem, a standardized EEG dataset is being developed by the Clinical Neurophysiology department of the University of Twente, following the example of research in computerized electrocardiogram interpretation [26, 10].

1.3 Research Goal

In this research we want to make a first step towards automated spike detection. The goal is to develop a method that supports encephalographers in the visual analysis of EEG recordings. At the moment every part of the recording is analysed, making it a time-consuming task. By detecting the events with an heightened chance of being an epileptiform discharge, we aim to reduce the time needed to analyse a record. This also supports the analysis of longer records, which improves the detection of evidence for epilepsy [17, 18].

1.4 Structure of the Report

Chapter 2 gives a theoretical framework, introducing the reader to, for example, electroencephalography. Wavelet analysis as spike detection method is discussed in Chapter 3. We propose to use matched filtering instead, a method treated in Chapter 4. The results using this method can be found in Chapter 5. The report finishes off with chapters 6 and 7 covering the conclusion and discussion of the presented work.

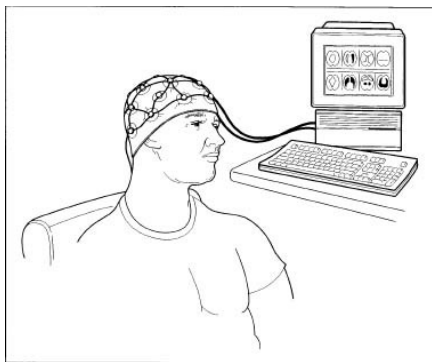
In this chapter some general background information is given. Section 2.1 introduces the reader to electroencephalography (EEG) and Section 2.2 to EEG in diagnosing epilepsy. Statistical measures such as sensitivity and specificity that are used in the evaluation of the performance of algorithms are defined in Section 2.3 and finally, preprocessing of the EEG record will be treated in Section 2.4.

2.1 Electroencephalography

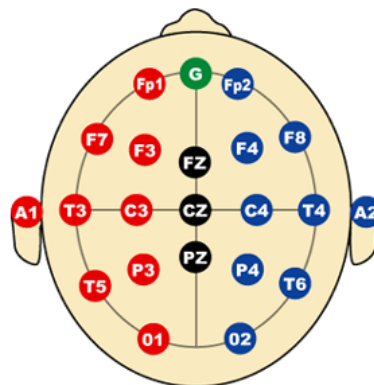
Electroencephalography (EEG) is a clinical tool used for the evaluation of brain function of patients. The EEG measures the electrical activity along the scalp, and is used in the diagnosis of, for example, coma, encephalopathy, brain death and plays an important role in the diagnosis of epilepsy [15].

Electrical activity of the brain is measured by electrodes placed on the scalp, such as shown in Figure 2.1. In this study the 10-20 electrode system is used, which is based on the general strategy of measuring the distance between two fixed anatomical points, such as the nasion (point where the bridge of the nose meets the forehead) and the inion (prominent point on the occiput), and then placing electrodes at 10% or 20% intervals along that line. Placement of electrodes in this system is shown in Figure 2.1b. The names of the electrodes identify with the lobe or area of the brain to which the electrode refers:

- F: frontal
- Fp: frontopolar
- T: temporal
- C: central



(a) Recording a user's brain waves using EEG [19].



(b) The 10-20 electrode system and the nomenclature of the EEG electrodes in the system. Note that the figure represents the head from above, with the nose on top and the earlobes on the left and right [19].

Figure 2.1: A typical EEG set up (top) and the 10-20 electrode system (bottom).

- P: parietal
- O: occipital
- A: aurical (ears)

Localisation is further narrowed down by numbering the electrodes. Even numbers stand for electrodes placed on the right side of the head, odd numbers for electrodes on the left. At last, the label z refers to points on the midline of the head [15].

Looking at an EEG recording, we do not see the ‘raw’ voltages measured, because these signals would be too electrically contaminated by the building’s electrical ground. We therefore use amplifiers which take two inputs, two electrodes for example. The second input is subtracted from the first and by that the contamination is cancelled out. The result is amplified and serves as the output. The concept is clarified by Figure 2.2.

The term *montage* refers to the order and choice of channels displayed on the EEG page. Most used montages are the *referential* and the *bipolar* montage. A referential montage compares each electrode to a reference point somewhere else on the body, a point which is hoped to be neutral. Such a reference point can be an electrode placed on the nose, chin, or earlobes, or is sometimes the common average of all scalp electrodes. In a bipolar montage each channel represents the voltage difference between two (adjacent) electrodes [15]. An example of an EEG page using a referential montage is shown in Figure 2.3. The length of the page is 10 seconds, which is typically used when analysing a record.

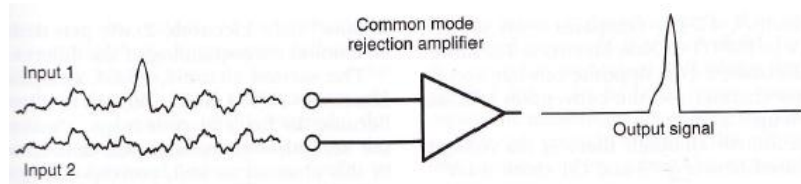


Figure 2.2: Example of an EEG amplifier with two inputs and its output. If we assume a bipolar montage, the two inputs could for example be the signals from electrodes $Fp1$ and $F3$. The output signal is then referred to as $Fp1 - F3$. The figure clearly demonstrates how electrical contamination is cancelled out using an amplifier [15].

2.2 Interictal Epileptiform Discharges

EEG is characterized by rhythmic background activity and short transients. These transients are not per definition signs of abnormal brain function. Transient features such as vertex waves and sleep spindles are seen in the EEG during normal sleep. Transients can also be caused by eyeblinks or movement of electrodes. Detection of spikes and sharp waves, however, may support the diagnosis of epilepsy.

Between seizures, the EEG of a patient with epilepsy may be characterized by occasional epileptiform transients, which consist of spikes or sharp waves having pointed peaks and last for 20-70 ms and 70-200 ms respectively. The detection of *interictal epileptiform discharges (IEDs)*, also referred to as *spikes*, is important since their presence is predictive of recurrent seizure in patients after first seizure [25] and is thus of use in making the diagnosis of epilepsy.

The first definition of a spike was introduced by Gloor in 1975 [7]. His definition of a spike:

1. a restricted triangular transient clearly distinguishable from background activity and having an amplitude of at least twice that of the preceding 5 seconds of background activity in any channel of EEG;
2. having a duration of < 200 ms;
3. including the presence of a field, as defined by involvement of a second adjacent electrode.

The International Federation of Societies for Electroencephalography and Clinical Neurophysiology describes interictal discharges as ‘a subcategory of epileptiform pattern, in turn defined as distinctive waves or complexes, distinguished from background activity, and resembling those recorded in a proportion of human subjects suffering from epileptic disorders’ [20]. The interictal discharges may be divided morphologically into sharp waves, spikes, spike-wave complexes and polyspike-wave complexes

The following definitions are used:

- *Sharp wave*; transient, clearly distinguishable from background activity, with pointed peak at conventional paper speeds and a duration of 70 to 200 milliseconds (ms);
- *Spike*; same as sharp wave, but with a duration of 20 to 70 ms;
- *Spike-wave complex*; pattern consisting of a spike followed by a slow wave;
- *Polyspike-wave complex*; same as spike-wave complex, but with two or more spikes associated with one or more slow waves.

Figure 2.3 gives an impression of how such a transient looks like on EEG. Some examples of sharp waves and spike-wave complexes are given in figures 2.4 and 2.5 (page 9).

In practice, it is not important that the distinction between the morphological differences of epileptiform discharge is made. The greatest challenge electroencephalographers face is to distinguish true epileptiform discharges from normal or nonspecific sharp transients and artifacts. Normal variants in the EEG that look like IEDs are for example vertex waves and K-complexes that occur randomly during sleep (Figure 2.6 on page 9). Artifacts or electrical disturbances can be caused by movements or eyeblinks (Figure 2.8 on page 13).



Figure 2.3: *This figure nicely illustrates the sudden appearance of an interictal epileptiform discharge on EEG (recording a0009672). The colored band marks a polyspike-wave complex.*

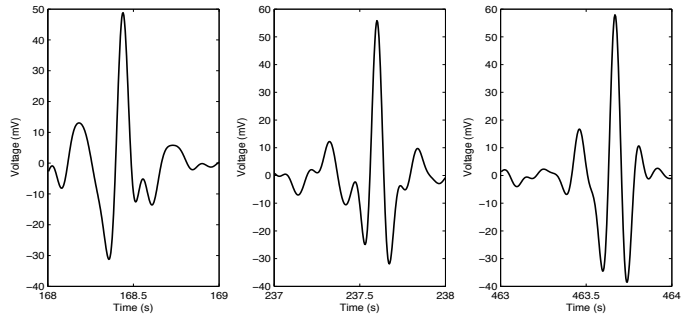


Figure 2.4: *Examples of sharp waves (taken from EEG recording a0006845).*

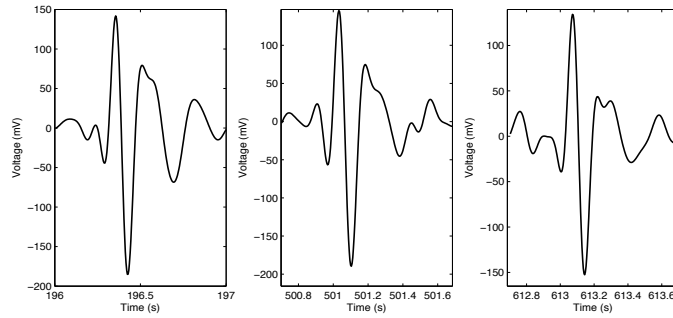


Figure 2.5: *Example of spike wave complexes (taken from the EEG recording a0009672).*

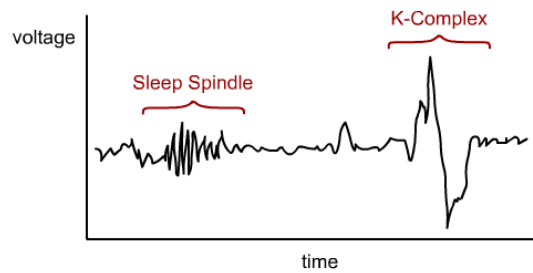


Figure 2.6: *K-complex; an EEG waveform that occurs randomly during sleep [21].*

2.3 Performance Measures

The performance of tests or algorithms is often measured using the statistical measures *sensitivity* and *specificity*. In the context of this study, the sensitivity is a measure of how likely the algorithms picks up an epileptiform discharge if present in the signal. Specificity is a measure of how likely it ‘ignores’ non-epileptiform parts of the signal. An ideal algorithm would have a sensitivity and specificity of 100 %; such an algorithm would perfectly mark all epileptiform discharges and nothing else.

2.3.1 Sensitivity and FPM

The sensitivity and specificity of an algorithm follow from the number of *True Positives (TP)*, *False Positives (FP)*, *True Negatives (TN)* and *False Negatives (FN)*. Each event that the algorithm correctly identifies as a spike is a true positive and each event that the algorithm should have neglected but was marked as spike instead, is a false positive. *TN* is the number of non-spike events in the recording that are neglected by the algorithm (as it should). Finally, the false negatives are the spikes in the recording that the algorithm did not detect as such. This classification is illustrated by Table 2.1. Notice that $TP + FN$ is the number of spikes known to be present in the recording, whereas $TN + FP$ is the number of non-epileptiform events. Likewise we see that $TP + FP$ is the number of events that the algorithm identifies as epileptiform (positive outcomes), whereas $FN + TN$ is the number of events the algorithm states to be non-epileptiform (negative outcomes).

		True state	
		<i>IED</i>	<i>non-IED</i>
Algorithm says	<i>IED</i>	TP	FP
	<i>non-IED</i>	FN	TN

Table 2.1: Classification of the outcomes of a spike detection algorithm in *True Positives (TP)*, *False Positives (FP)*, *True Negatives (TN)* and *False Negatives (FN)*.

The sensitivity follows as the probability of a positive outcome given an epileptiform discharge is present, i.e.

$$\begin{aligned}
 \text{Sensitivity} &= P(\text{identifies IED} \mid \text{IED present}) \\
 &= \frac{TP}{TP + FN}
 \end{aligned} \tag{2.1}$$

Likewise the specificity follows as the probability of a negative outcome, given a non-epileptiform event takes place:

$$\begin{aligned}
 \text{Specificity} &= P(\text{identifies non-IED event} \mid \text{IED not present}) \\
 &= \frac{TN}{TN + FP}
 \end{aligned}$$

For online applications it is useful to know how often the system gives a false alarm. That is why the specificity is often replaced by the *False Positive Rate (FPR)* defined as

$$\text{FPR} = \frac{FP}{FP + TN} = 1 - \text{specificity}$$

. or the *False Positives per Minute* defined as

$$\text{FPM} = \frac{FP}{\text{length file (min)}} \quad (2.2)$$

In this study we will mostly use the sensitivity and FPM as performance measures.

2.3.2 ROC curve

The *Receiver Operator Characteristic (ROC) curve* was introduced in World War II military radar operations as a way to visualize the operators' ability to identify friendly or hostile aircraft based on a radar signal. The operators could not afford identifying a hostile aircraft as friendly by mistake, but at the same time their resources were limited; they were not able to intercept all aircraft. The ROC curve was introduced as a graphical tool to explore the trade-offs between these two losses at various decision thresholds when a quantitative variable is used to guide the decision [4].

The ROC curve found its way into signal detection studies and is still used a lot in the evaluation of diagnostics systems. The sensitivity and false positive rate are the conflicting interests; we want to maximize the sensitivity and at the same time minimize the false positive rate. A typical ROC curve is shown in Figure 2.7.

ROC curves help us to compare different threshold settings or algorithms.

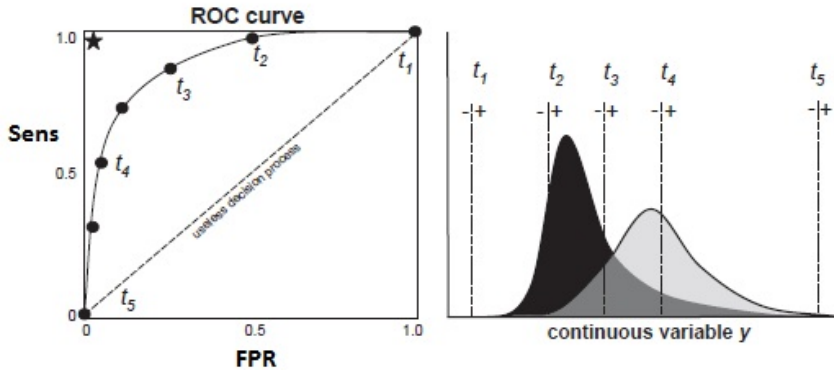


Figure 2.7: Left we see the ROC curve corresponding to the events described on the right. t_1 - t_5 represent thresholds for the variable y , which for example represents the number of flu antibodies present in the blood. If the threshold is low (t_1), we find all true flu cases (light blob), but also many false flu detections (dark blob). If the threshold is high (t_5), none of the blood samples tests positive for flu. The optimal point is the upper left star representing a sensitivity of 1 with an FPR of 0 [4].

2.4 Preprocessing

2.4.1 Filtering

Epileptiform discharges are known to correspond to the frequency band of 4-32 Hz [11]. Events corresponding to a frequency $< 4\text{Hz}$ or $> 32\text{Hz}$ are therefore not of interest for us and we might as well leave them out of our analysis. We will therefore use a bandpass filter that passes frequencies within a certain range and rejects frequencies outside that range. The bandpass filter used is the 4th order Butterworth filter with cut-of frequencies of 4 and 20Hz. The upper limit of 20Hz is chosen as to minimize the presence of myogenic artifacts that are known to lie in the 20 – 30Hz frequency band.

2.4.2 Eyeblinks

An EEG signal often contains eye-related artifacts such as eyeblinks. Eyeblinks are characterized by positive deflections in the most anterior electrodes and are explained by an upward rotation of the eyeball during the lid closure. The eyeball acts as a dipole with a positive pole oriented anteriorly (cornea) and a negative pole oriented posteriorly (retina). When the eye rotates, it generates a large-amplitude alternate current field, which is detectable by any electrodes near the eye (usually electrodes Fp1 and Fp2) [3]. An example of eyeblinks in the EEG is shown in Figure 2.8.

Typically an EEG recording not only contains signals from electrodes placed on the head, but also an *electrocardiography (ECG)* signal (from the heart), reference signals from electrodes placed on, for example, the earlobes and an *electrooculography (EOG)* signal. This last signal is shown in Figure 2.8 (channel *Cb2*) and corresponds to the resting potential of the retina. This signal thereby correlates well with eyeblink events, which is illustrated in the figure. The *EOG*-channel can therefore be used to filter the signal for eyeblink artifacts. The results of such a preprocessing operation using the method of Lodder [16] are shown in Figure 2.9. This method uses *Independent Component Analysis (ICA)* to find the correlation between the EEG signals and the *EOG*-channel. The highest correlating component is removed and with the reverse transform the signal is recovered, which is then assumed to be free of eyeblink artifacts.

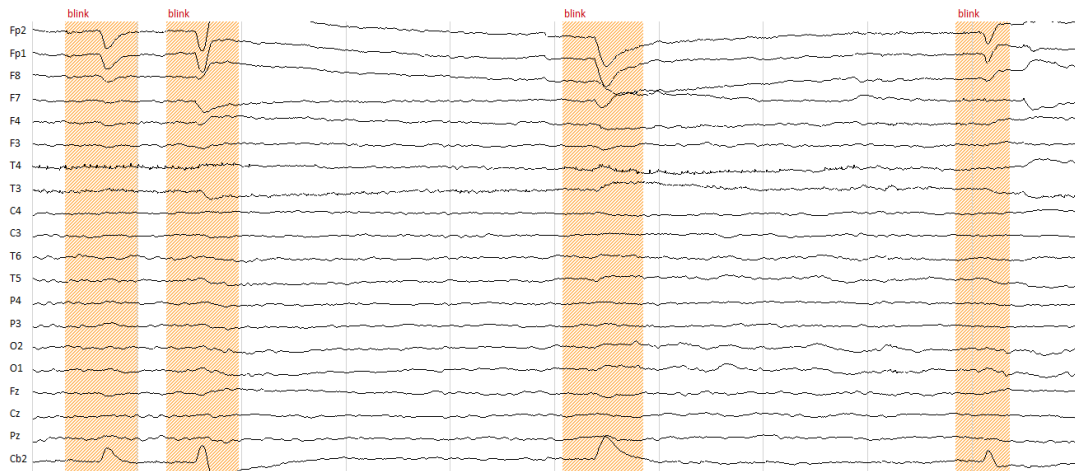


Figure 2.8: Referential montage showing transients caused by eyeblinks (marked parts). We clearly see a correlation between the transient behaviour in channels Fp1 and Fp2 and the EOG-channel (in this file named Cb2).

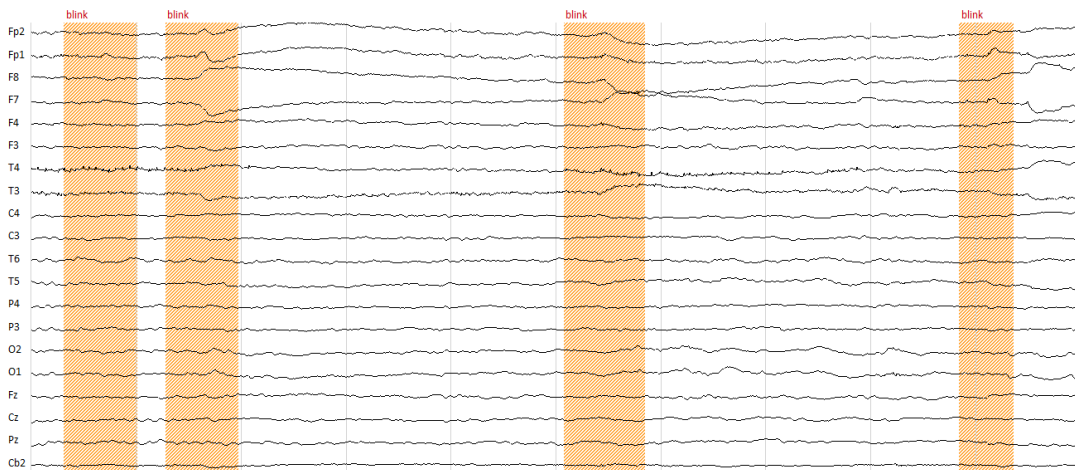


Figure 2.9: The EEG of Figure 2.8 after preprocessing on eyeblink artifacts. We see the same 10 seconds of EEG are now free of transients.

Fourier analysis has proven to be very successful in many signal processing applications. It describes a phenomenon (signal), $x(t)$ as a superposition of harmonic basis elements $\hat{x}(f)e^{i2\pi ft}$. A note (as in musical notation), for example, is described as a superposition of its fundamental frequency and its higher harmonics.

A drawback of Fourier is that these basis elements are not local in time and as such are not useful if temporal change is important. Temporal change is for example important in music; the music scores describe a song: they specify *when*, for how *long* and at which *pitch* (frequency) a note should be played.

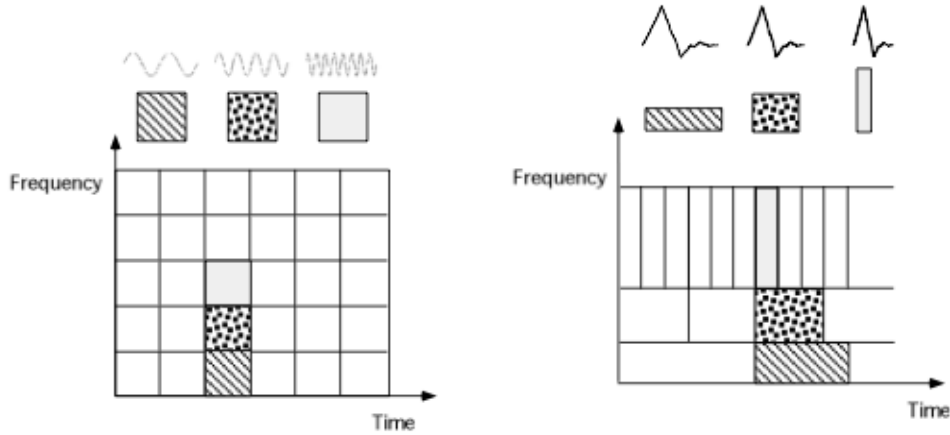
Another limitation of Fourier is that the time and frequency resolution, T_r and f_r , are the same throughout the time-frequency plane. We can improve the frequency resolution, but then the time resolution becomes worse and vice versa. This is illustrated in Figure 3.1a.

A well known alternative to the harmonic basis elements are *wavelets*. Wavelets allow multiresolutional analysis, meaning that T_r and f_r need not be the same throughout the time-frequency plane (Figure 3.1b).

In wavelet analysis the concept *scale* is used, instead of frequency. It is a useful property of signals and images. For example, we can analyse temperature data for changes on different scale; day-to-day, year-to-year or decade-to-decade. Scale and frequency are related though. On a small scale (the day-to-day temperature changes) we look at details, which relates to a high frequency. On a large scale, slowly changing features are examined, i.e., we analyse at a low frequency.

3.1 An introduction to wavelet analysis

In this section the basic idea of wavelet analysis is shown by working out an example. The idea is that a signal x is repeatedly separated in what is called an



(a) Fourier basis functions, time-frequency tiles, and coverage of the time-frequency plane.

(b) Daubechies wavelet basis functions, time-frequency tiles, and coverage of the time-frequency plane. Low frequency events need a large time frequency resolution but have small frequency resolution.

Figure 3.1: Differences in time-frequency resolutions for Fourier and Wavelet analysis [8].

approximation component $a(t)$ and a detail component $d(t)$. By this, local behaviour (detail) can be separated from long-term behaviour (approximation). It separates the low-frequency from the high-frequency content. Take the example of temperature measurements, where the high-frequency components represent day-to-day changes and low-frequency components represent seasonal changes.

Suppose we have a discrete signal $x_n = [x_0 \ x_1 \ \dots \ x_{N-1}] \in \mathbb{R}^N$ with $N = 2^L$ samples as shown in Figure 3.2.

The approximation and detail coefficients are defined as the pairwise average and difference:

$$a_n^1 := \frac{1}{2}[x_0 + x_1 \ x_2 + x_3 \ \dots \ x_{N-2} + x_{N-1}] \in \mathbb{R}^{\frac{N}{2}} \quad (3.1)$$

$$d_n^1 := \frac{1}{2}[x_0 - x_1 \ x_2 - x_3 \ \dots \ x_{N-2} - x_{N-1}] \in \mathbb{R}^{\frac{N}{2}} \quad (3.2)$$

Figure 3.3 shows the approximation a_n^1 which roughly looks like the original signal x_n , and the detail coefficients, d_n^1 . The detail coefficients reveal that the difference between two consecutive points is small, except where x_n jumps.

We have obtained a_n^1 and d_n^1 from x_n by the following mapping:

$$x_n \in \mathbb{R}^N \rightarrow (a_n^1, d_n^1) \in (\mathbb{R}^{\frac{N}{2}}, \mathbb{R}^{\frac{N}{2}})$$

This mapping is invertible for all even N (note that then x_n has as many samples as (a_n^1, d_n^1)).

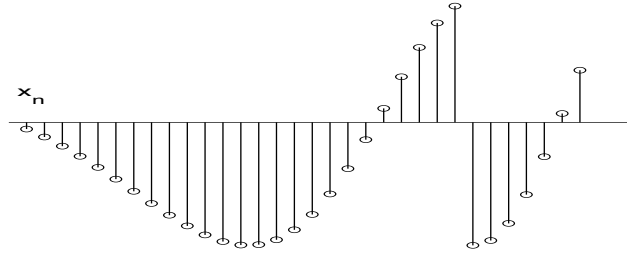


Figure 3.2: Discrete signal $x_n \in \mathbb{R}^{32}$.

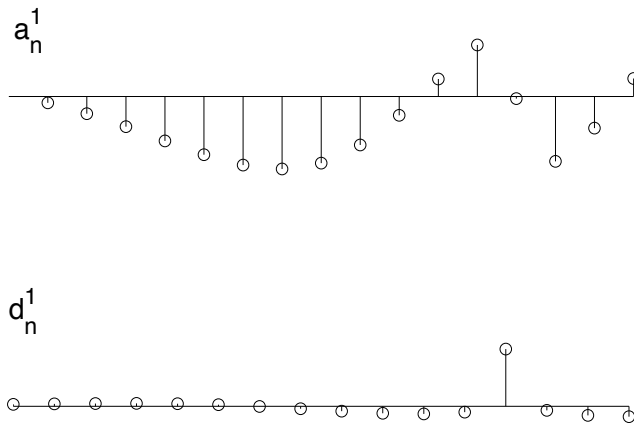


Figure 3.3: First level approximation a_n^1 (top) and detail coefficients d_n^1 (bottom) of the discrete function x_n of Figure 3.2.

We can take the first-level approximation a_n^1 , and decompose it in the same manner to obtain the second-level approximation a_n^2 and corresponding detail coefficients d_n^2 :

$$a_n^1 \rightarrow (a_n^2, d_n^2)$$

We can continue this process upto $(a_n^L, d_n^L) \in (\mathbb{R}^1, \mathbb{R}^1)$:

$$\begin{aligned} a_n^2 &\rightarrow (a_n^3, d_n^3) \\ a_n^3 &\rightarrow (a_n^4, d_n^4) \\ &\vdots \\ a_n^{L-1} &\rightarrow (a_n^L, d_n^L) \end{aligned}$$

Each mapping results in a coarser approximation of x_n (each step the time resolution decreases, and the frequency resolution increases with a factor 2). As each mapping is reversible, we can reconstruct x_n uniquely from the final approximation a_n^L and all detail levels:

$$(a_n^L, d_n^L, d_n^{L-1}, \dots, d_n^1) \rightarrow x_n$$

For $x_n \in \mathbb{R}^N$ (Figure 3.2) the total decomposition is shown in Figure 3.4 (page 18).

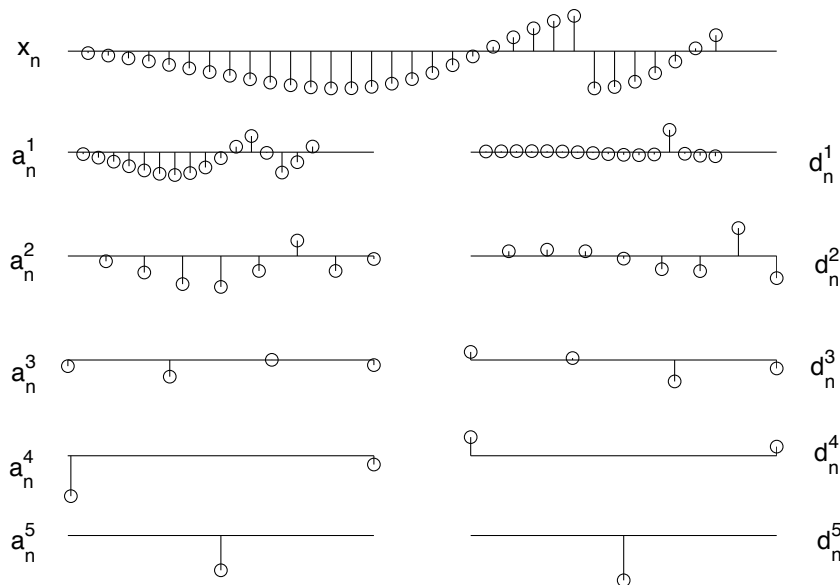


Figure 3.4: Complete decomposition of the discrete signal x_n . On top we have x_n and underneath the approximation (left) and detail components (right) from scales 1 upto 5.

3.1.1 Preserving norm

The idea of the ‘size’ of a signal is important in many applications. We would like to know how much electricity can be used in a defibrillator without ill effects, for instance. It is also good to know if the signal driving a set of headphones is strong enough to create a sound. For this reason, it is convenient to quantify this idea of ‘size’. The energy of a signal, defined as

$$E_x := \|x\|^2 \tag{3.3}$$

with $\|\cdot\|$ the Euclidean norm

$$\|x\| := \sqrt{\sum_{n=0}^{N-1} |x_n|^2} \quad (3.4)$$

is such a quantification. To be able to use this quantification in wavelet analysis, the wavelet measure needs to preserve energy. This means we need

$$|x_n|^2 = |a_n^L(x)|^2 + \sum_{i=1}^L |d_n^i(x)|^2$$

With the approximations and details defined as in (3.1) and (3.2) the norm is not preserved. Suppose for example the signal is constant, implying all detail coefficients to be zero. Then we have

$$|a_n^L(x)|^2 + \sum_{i=1}^L |d_n^i(x)|^2 = \frac{1}{2}|x_n|^2$$

If we simply multiply the wavelet transformation $x_n \rightarrow (a_n^L, d_n^L, d_n^{L-1}, \dots, d_n^1)$ by a factor $\frac{1}{2}\sqrt{2}$ the transformation from x_n is norm preserving.

3.1.2 Orthogonality

The wavelet transformation $x \rightarrow (a^1, d^1)$ can also be looked at as the expansion of x in the orthonormal basis $\phi_{0,k}, \psi_{0,k}$ with $k = 0, \dots, \frac{N}{2} - 1$ (see Figure 3.5). That is to say

$$\begin{aligned} d_k^1 &= \langle x, \psi_{0,k} \rangle \\ a_k^1 &= \langle x, \phi_{0,k} \rangle \end{aligned}$$

For every $\psi_{0,k}, \phi_{0,k}$ we have two neighbouring nonzero entries, all of its other entries being zero. Moreover, the $\psi_{0,k}$ do not overlap, which is also the case for the $\phi_{0,k}$.

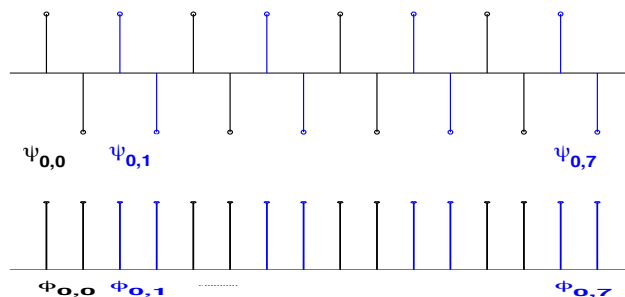


Figure 3.5: An orthonormal basis $\phi_{0,k}$ (top), $\psi_{0,k}$ (bottom).

Therefore, it is clear that these are orthogonal to each other. The same holds for the wavelet functions corresponding to the transformations from $a^1 \rightarrow (a^2, d^2)$ upto $a^{L-1} \rightarrow (a^L, d^L)$.

The $\psi_{0,0}$ is the so-called *mother wavelet*, $\phi_{0,0}$ the *scaling function* and the numbers d_k^m the *wavelet coefficients*.

3.2 Continuous-time wavelet transform

The previous section actually introduces one of the well known mother wavelets, namely the *Haar wavelet*. The continuous-time version is

$$\psi(t) := \begin{cases} 1 & t \in [0, \frac{1}{2}) \\ -1 & t \in (\frac{1}{2}, 1] \\ 0 & \text{else} \end{cases}$$

with scaling function

$$\phi(t) := \begin{cases} 1 & t \in [0, 1) \\ 0 & \text{else} \end{cases}$$

The basis functions that are used in wavelet analysis are all scaled and translated versions of the chosen mother wavelet and scaling function. They are obtained as follows

$$\begin{aligned} \psi_{j,k}(t) &:= \frac{1}{\sqrt{2^j}} \psi\left(\frac{t-k}{2^j}\right), \quad j = 0, 1, \dots, \quad k = 0, 1, \dots, 2^j - 1 \\ \phi_{j,k}(t) &:= \frac{1}{\sqrt{2^j}} \phi\left(\frac{t-k}{2^j}\right), \quad j = 0, 1, \dots, \quad k = 0, 1, \dots, 2^j - 1 \end{aligned}$$

where j stands for the scale and k for the translation. The functions obtained form an orthonormal sequence. A part from the Haar wavelet sequence is given in Figure 3.6 (page 21).

At each scale j , the expansion of x_n will be determined in the orthonormal basis $\phi_{j,k}, \psi_{j,k}$. The results of this expansion are the approximation (derived via the expansion in the scaling function or averaging filter $\phi_{j,k}$) and the *wavelet coefficients* d_j^k (via the expansion in the wavelet $\psi_{j,k}$).

The Haar wavelet is one of many wavelet transforms. Figure 3.7 (page 21) shows the mother wavelets of some other well known ones.

3.3 Applications of wavelet analysis

Wavelet analysis is used in many fields. To get an idea: astronomy, acoustics, nuclear engineering, sub-band coding, signal and image processing, neurophysiology, music, magnetic resonance imaging, speech discrimination, optics, fractals, turbulence, earthquake-prediction, radar, human vision, and in pure mathematics applications such as solving partial differential equations [9]. A few of them are discussed in the following.

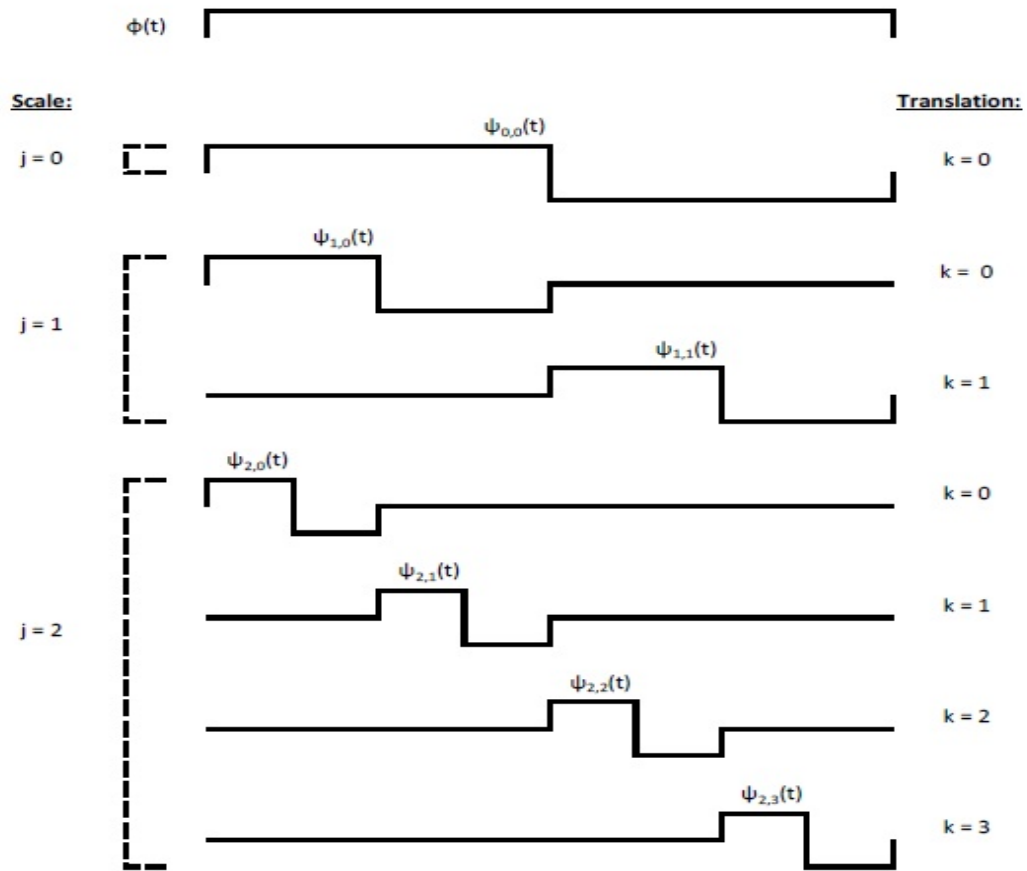


Figure 3.6: Haar wavelet sequence for scales $j = \{0, 1, 2\}$ and corresponding translations k .

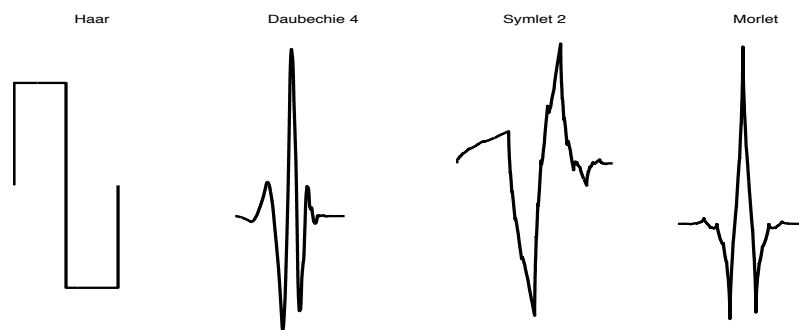


Figure 3.7: From left to right: the Haar, Daubechie 4, Symlet 2 and Morlet mother wavelet.

3.3.1 Data reduction

Wavelet analysis is a very effective data reduction tool and is successfully used in for example the storage of finger prints [9]. In the years 1924-1995 the FBI collected about 30 million fingerprints. These were almost all inked impressions on paper cards. Digitalizing these cards was an issue, since one set of finger prints would need about 0.6 MB to store. In total the FBI had about 200 TB of data to store which was very expensive; data compression was needed. Wavelet analysis was used to do so. Decomposition the picture (the fingerprint), and storing the last approximation coefficients with all detail coefficients would almost decrease the storage capacity needed by a factor two. If besides that also the smallest detail coefficients are put to zero, much less data is needed to store a single fingerprint. The difference in the actual fingerprint and the one reconstructed from the left-over wavelet coefficients could only be seen by experts.

3.3.2 Denoising

Wavelet analysis can also be used to denoise signals. In Figure 3.8 we see an example taken from the MATLAB wavelet GUI. On the left we see a noisy signal, on the right the result of wavelet reconstruction after putting almost 95% of the smallest detail coefficients to zero.

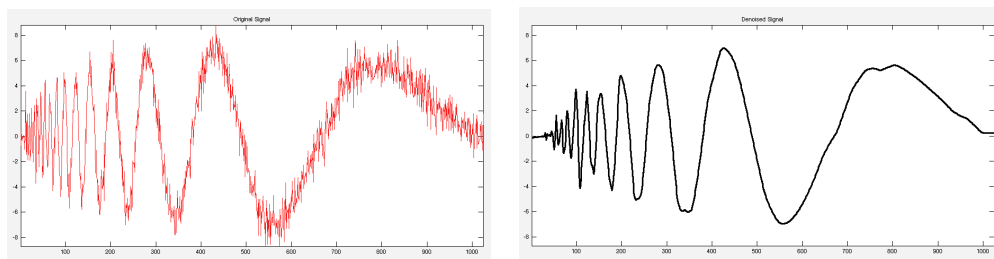


Figure 3.8: *Wavelet example taken from the MATLAB GUI demonstrating the strength of wavelet analysis in denoising signals.*

3.3.3 Feature extraction

Wavelet analysis is a good tool in feature extraction, provided that a suitable mother wavelet can be found. For this extraction, again, the value of the wavelet coefficients is important. The higher the wavelet coefficient d_j^k , the better the signal (locally) looks like the scaled and dilated wavelet ψ_j^k . The Haar wavelet can, for example, be used to detect a discontinuity as in Figure 3.2. The Daubechie 4 wavelet is used in the detection of epileptiform spikes [11], because the wavelet kind of looks like one (Figure 3.9).

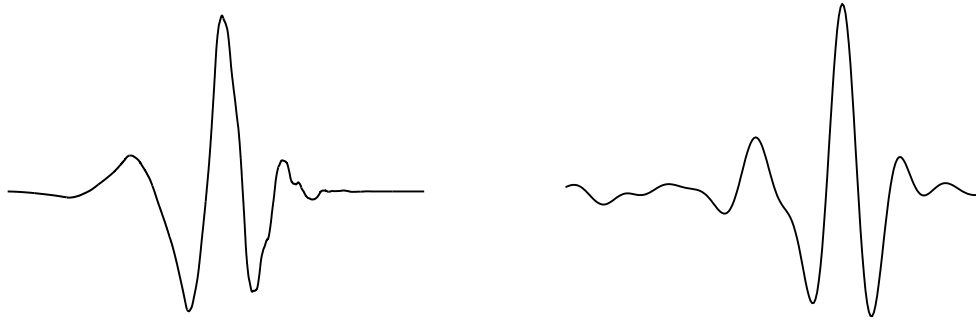


Figure 3.9: *Daubechie 4 mother wavelet (left) and a true epileptiform spike taken from EEG recording a0006845 (right).*

3.4 Wavelet analysis in spike detection

Wavelet analysis was used in several studies in which automatic spike detection was the main goal [11, 5, 14, 22, 13, 23]. In almost all the studies the sensitivity is high, sometimes even above 90%. Kalayci and Ozdamar [13] combined wavelets and neural networks and obtained a sensitivity of 90.8% and a specificity of 93.2%. Senhadji et al. [23] combined a parametric approach with wavelet analysis and obtained a sensitivity of 86%.

Most recent is the study from Indiradevi et al [11]. To get a feeling for wavelet analysis in spike detection we implemented their approach ourselves. Their approach will be explained in Section 3.4.1 and Section 3.4.2 reports on our findings after implementation of the approach.

3.4.1 The approach of Indiradevi et al. [11]

The data used in this research were 256 Hz sampled EEG signals, which were band pass filtered (as explained in Section 2.4), using the [0.5 – 100] Hz frequency band. The signal consisted of 18 channels from a referential montage, namely *Fp1*, *Fp2*, *F3*, *F4*, *C3*, *C4*, *P3*, *P4*, *F7*, *F8*, *T1*, *T2*, *T3*, *T4*, *T5*, *T6*, *O1* and *O2*.

The wavelet transform used was the Daubechie 4 wavelet (Figure 3.9). This wavelet was chosen from all wavelet candidates (the wavelets available in the MATLAB toolbox) as it scored highest in cross-correlation with a known epileptic discharge.

Actual detection of spikes was based on the fact that the optimal resolution to analyse IEDs corresponds to the frequency band 4-32 Hz. Therefore a discrete wavelet decomposition was performed upto level 6. The wavelet coefficients of levels 4 and 5, corresponding to a frequency band of 4-16 Hz, are chosen in the analysis so as to minimize the contribution of non-epileptiform high frequency events partly overlapping in the 20-30 Hz frequency band.

An epileptiform event is looked for in every channel and is considered found if the squared reconstructed detail coefficients at scale 4 or 5 exceed a threshold. This threshold is an adapted threshold defined as

$$T_j := T \cdot 2^j \quad (3.5)$$

Here j stands for the scale and T is defined as:

$$\begin{aligned} T &:= \frac{C \cdot H_{j,k}}{\Delta\psi}, \text{ with:} \\ C &:= \text{the average value of standard deviation of 18 channels} \\ H_{j,k} &:= \text{reconstructed wavelet coefficients for scale } j \\ \Delta\psi_j &:= \max(\psi_j) - \min(\psi_j) \end{aligned}$$

We should think of T_j as a kind of ‘moving’ threshold. T_j is an array of thresholds: each time instance n has its own threshold.

Results

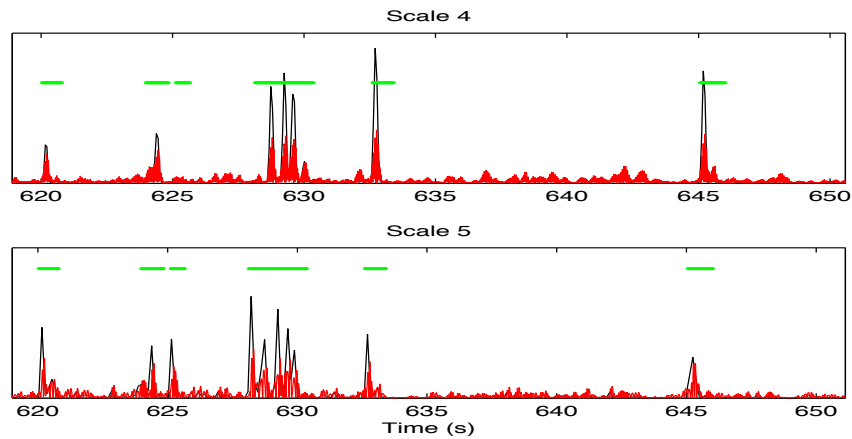
Indiradevi et al. obtained a sensitivity of 91.7% and a specificity of 89.3% following this approach. The reported limitations of the method: it has difficulties detecting small amplitude spikes, picks up quite some artifacts and fails to detect spikes when the amplitude of the slow wave that follows the spike exceeds the spikes amplitude [11].

3.4.2 Own implementation, results and conclusion.

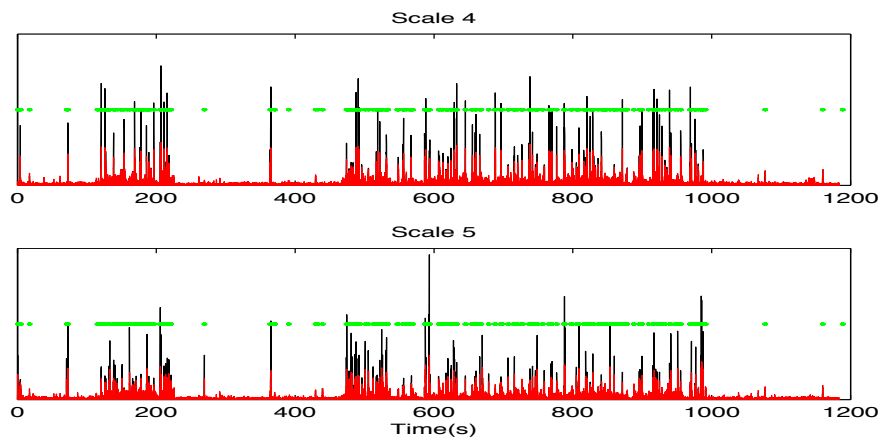
We implemented the method of Indiradevi et al. [11] and tested it on the 250 Hz sampled file a0009672, using the 19 channels $Fp1$, $Fp2$, $F3$, $F4$, $C3$, $C4$, $P3$, $P4$, $F7$, $F8$, $T3$, $T4$, $T5$, $T6$, $O1$, $O2$, Fz , Cz and Pz that were at our disposal. We tried to visualise the approach in figures 3.10a and 3.10b (page 25). To obtain these figures we had to replace the squared reconstructed wavelet coefficients, that were originally used by Indiradevi et al., by the squared detail coefficients. Figure 3.10 shows the results for a 30s part of the file. We see that the squared detail coefficients (in black) in most cases exceed the threshold (red) at the point where a spike is known to be present (green). In Figure 3.10b we see the results for the complete file.

No performance measures were determined. The figures seem to imply satisfactory results, but the fact that the choice for a template is bounded by wavelets is not. The Daubechie 4 wavelet looks like an epileptiform discharge, but that is a lucky coincidence. Besides that, its form is not like *all* epileptiform discharges known. Moreover, orthogonality and invertibility of wavelets are necessary for the interpretation of the value of the detail coefficients, but are intuitively of no relevance for the presence or absence of a spike. Correlation and the fact that we work with discrete wavelets (discrete in time/scale), are relevant features though. These features, however, are

also captured by *matched filtering*. A big advantage of matched filtering is the freedom in the choice of templates. Moreover, the time resolution in wavelet analysis is still bounded by the frequency resolution. The matched filter is a moving average convolution filter. This makes we have a correlation coefficient at our disposal at each time instance (sample) n . Chapter 4 discusses matched filtering and how it can be used in spike detection.



(a) Results for a 30s part of file a0009672.



(b) Results for file a0009672.

Figure 3.10: Results of the implementation of the method of Indiradevi on file a0009672 for a 30s part of the record. The top part of each figures gives the results for level 4, below the results for level 5. In black we have the squared detail coefficients, in red the adapted threshold and in green the annotations.

3.5 Summary

Fourier analysis has proven its worth over the years, but has the disadvantage that it has a fixed time-frequency resolution and is not local in time. Wavelet analysis overcomes these problems; it is multiresolutional and local in time as is clarified by Figure 3.11.

An expansion of x is determined for the orthonormal bases $\psi_{j,k}$ and $\phi_{j,k}$, which are scaled ($j = 0, 1, \dots$) and dilated ($k = 0, 1, \dots, 2^j - 1$) versions of the mother wavelet $\psi_{0,k}$ and the scaling function $\phi_{0,k}$. At each scale this results in an approximation (via the expansion in $\phi_{j,k}$) and the wavelet coefficients d_j^k (through $\psi_{j,k}$).

There are a lot of different mother wavelets $\psi_{0,n}$. The choice for a particular wavelet should be based on the intended application. The Daubechie 4 wavelet is for example used in the detection of spikes in EEG [11].

Indiradevi et al. [11] used wavelet analysis for automated detection of spikes in EEG, which led to a sensitivity of 91.7% and a specificity of 89.3%. Matched filtering, however, seems to have the potential to perform better. This will be investigated in Chapter 4.

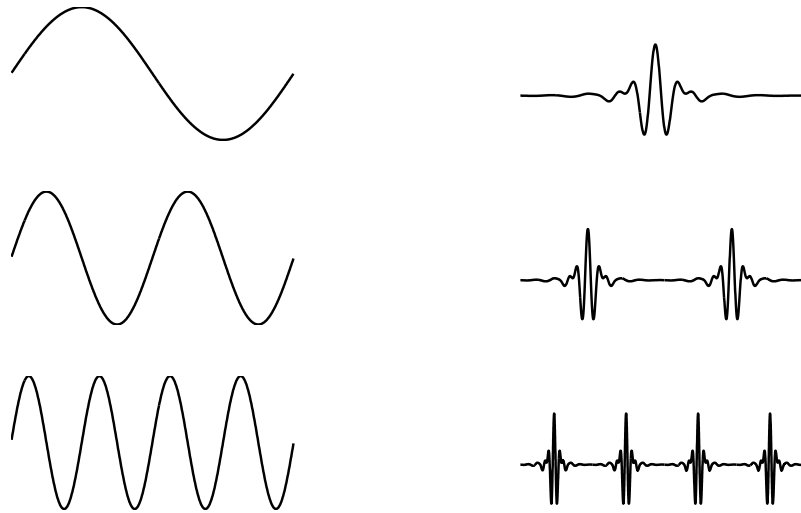


Figure 3.11: *The Fourier basis elements are local in frequency, but give no local information (when is a certain frequency present?). In wavelet analysis we can do both, as can be seen on the right for the Meyer wavelet.*

Matched filtering is used to detect the presence of known signals, *templates*, in a signal that is contaminated by noise. An example is radar, where we want to determine the distance of an object by reflecting a known signal off it. The received signal is assumed to be a scaled and phase-shifted form of the transmitted signal, with added noise. To determine the distance of the object, the received signal is correlated with a matched filter which is a copy of the transmitted signal. When the correlation coefficient exceeds a certain threshold we can conclude with high probability that the transmitted signal has been reflected off the object (Figure 4.1 on page 28). Since we know the speed of propagation and the time between transmitting and receiving we can estimate the distance of the object.

This chapter will discuss the theory of matched filtering and shows how matched filtering can be used for the detection of epileptiform discharges in EEG.

4.1 Theory of Matched Filtering

Suppose we have a time series $\{u_n\}_{n \in (1, \dots, N)}$, which for example is a single channel EEG signal. We assume the data is a superposition of background x_n and spike waveform w_n , i.e. $u_n = x_n + w_n$. At each time n we would like to explain the data over the preceding $(M + 1)$ samples,

$$U_n := (u_{n-M}, u_{n-M+1}, \dots, u_n) \in \mathbb{R}^{1 \times (M+1)}$$

as much as possible by a given spike template

$$V := (v_0, \dots, v_M) \in \mathbb{R}^{1 \times (M+1)}$$

which we can do by choosing $\theta_n \in \mathbb{R}$ such that

$$U_n = \theta_n V + X_n$$

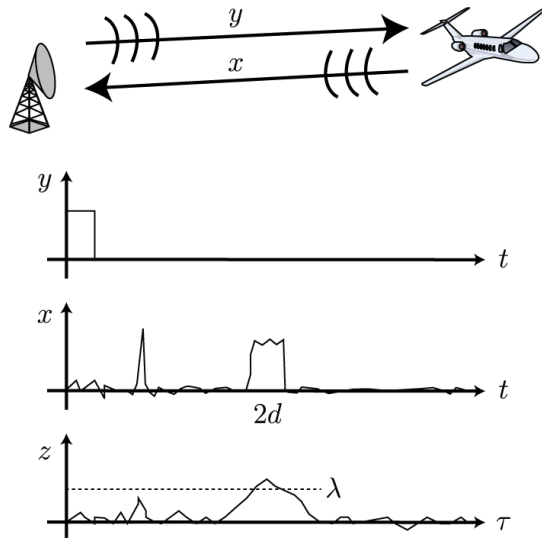


Figure 4.1: The pulse y reflects off a target and returns to the antenna as signal x . Matched filtering, with y as template, gives us z and allows us to determine the distance of the target [2].

with minimal contribution of the background $X_n \in \mathbb{R}^{1 \times (M+1)}$.

One way to do this is by solving

$$\theta_n^* = \arg \min_{\theta_n \in \mathbb{R}^1} \|U_n - V\theta_n\|$$

with $\|\cdot\|$ the Euclidean norm as defined by (3.4).

It is a classic result that θ_n^* satisfies (4.1) if and only if θ_n^* satisfies the *normal equations* $VV^T\theta_n^* = U_nV^T$ with V^T the transpose of V . Since VV^T is invertible this yields

$$\theta_n^* = \frac{V}{\|V\|^2} U_n^T \quad (4.1)$$

This is the classic matched *finite impulse response (FIR) convolution* filter with input U_n and output θ_n^* ,

$$\theta_n^* = h_0u_n + h_1u_{n-1} + \dots + h_Mu_{n-M}, \quad \text{with } h := V$$

We see that the best approximation of U_n is given by: $U_n^* = \theta_n^*V$. This best approximation is unique and we think of it as the part of U_n that is explained by the template. The remaining background follows as

$$\widetilde{X}_n = U_n - \theta_n^*V$$

4.1.1 Expectation and Variance of θ_n^*

Under the assumption that $u_n = w_n + x_n$ with x_n zero mean white noise and w_n a known deterministic signal (the ‘spike behaviour’), we will derive the expectation and variance of θ_n^* . These numbers will give us an idea of the performance of the matched filter. We can find out for example, how big an influence the white noise or the number of samples of the template has. The expectation of θ_n^* , $\mathbb{E}(\theta_n^*)$, equals

$$\begin{aligned}\mathbb{E}(\theta_n^*) &= \mathbb{E}\left(\frac{V}{\|V\|^2} U_n^T\right) \\ &= \frac{V}{\|V\|^2} W_n^T \\ &= \begin{cases} 1 & \text{if } W_n = V \\ 0 & \text{if } W_n = 0 \end{cases}\end{aligned}\quad (4.2)$$

We see $\mathbb{E}(\theta_n^*) = 1$ if the spike behaviour W_n and the template V are equal to each other and $\mathbb{E}(\theta_n^*) = 0$ if no spike behaviour is present. It also follows that $\mathbb{E}(\theta_n^*) = 2$ if the spike behaviour equals twice the template V . We can therefore think of θ_n^* as a linear correlation coefficient.

With known $\mathbb{E}(\theta_n^*)$ we can derive the variance of θ_n^* follows as

$$\begin{aligned}\text{var}(\theta_n^*) &= \mathbb{E}[(\theta_n^* - \mathbb{E}(\theta_n^*))^2] \\ &= \mathbb{E}\left[\left(\frac{V}{\|V\|^2} U_n^T - \frac{V}{\|V\|^2} W_n^T\right)^2\right] \\ &= \mathbb{E}\left[\left(\frac{V}{\|V\|^2} X_n^T\right)^2\right] \\ &= \frac{\sigma_x^2}{\|V\|^2} \\ &= \frac{\sigma_x^2}{(M+1)P_V}\end{aligned}\quad (4.3)$$

with σ_x^2 the variance of the white noise X_n , and P_V the power of the template, which is the time average of the energy (Definition (3.3)), i.e.

$$P_V = \frac{\|V\|^2}{(M+1)}$$

We see that the white noise influences the variance of θ_n^* . The noisier the signal ($> \sigma_x^2$), the larger the variance of θ_n^* . We also see that the more samples in the template ($> M$), the smaller the variance. This seems logical: suppose that for template A, $M = 2$ and for template B, $M = 200$. The probability that white noise will resemble template A at some time t is significantly larger than the possibility that it will resemble template B. Finally we can remark that an increase in the power of the template, decreases the variance of θ_n^* .

4.2 Ratio of Powers

The vector θ_n^* that follows from the matched filter gives us an indication for the presence of the template V . If $\theta_n^* = 1$, it seems that we have found the presence of the event we are looking for. However, θ_n^* does not give information on how much of the signal power is explained by the template. For $\theta_n^* = 1$ we may at the same time find only 20% of the signal power being explained by the template, for example when $\sigma_x^2 \gg \|V\|^2$. If we know how much of the signal power can be explained by the template, this helps us in the decision whether or not we have found a spike candidate.

We will therefore take the difference of the signal power and the power of the ‘template part’ into account as well. We define this difference, P_n^{rest} , as

$$P_n^{\text{rest}} := \frac{\|U_n - \theta_n^* V\|^2}{(M+1)} = \frac{\|U_n\|^2 - (\theta_n^*)^2 \|V\|^2}{(M+1)}$$

The expected value of P_n^{rest} is follows as

$$\begin{aligned} (M+1) \mathbb{E}(P_n^{\text{rest}}) &= \mathbb{E} [\|U_n\|^2 - (\theta_n^*)^2 \|V\|^2] \\ &= \mathbb{E} [\|X_n + W_n\|^2 - (\theta_n^*)^2 \|V\|^2] \\ &= \mathbb{E} [\|W_n\|^2 + \|X_n\|^2] - \mathbb{E} [(\theta_n^*)^2 \|V\|^2] \\ &= [\|W_n\|^2 + (M+1)\sigma_x^2] - \|V\|^2 [\text{var}(\theta_n^*) + \mathbb{E}(\theta_n^*)^2] \\ &= [\|W_n\|^2 + (M+1)\sigma_x^2] - \left[\sigma_x^2 + \frac{(VW_n^T)^2}{\|V\|^2} \right] \\ &= M\sigma_x^2 + \|W_n\|^2 - \frac{(VW_n^T)^2}{\|V\|^2} \end{aligned}$$

Now if W_n is equal to (a scaled version of) V , i.e. $W_n = \alpha V$ we get

$$\mathbb{E}(P_n^{\text{rest}}) = \sigma_x^2 \left(1 - \frac{1}{M+1} \right) \quad (4.4)$$

We remark that a noisy signal (large σ_x^2) makes it difficult to explain the power of the signal with the template; more power remains unexplained. Notice also that the expected value does not depend on the power of the template, but on the number of samples in the template. The more samples, the smaller the probability that the noise resembles the template. Notice also that $\mathbb{E}(P_n^{\text{rest}}) < \sigma_x^2$. The template thus always matches with a part of the noise as well. At last we see that if $M = 0$, i.e. our template exists of just one sample, $\mathbb{E}(P_n^{\text{rest}}) = 0$. This makes perfect sense because every signal sample is then equal to the (scaled) template.

In this study we will use the *Ratio of Powers* (notation R_n), a normalised version

of P_n^{rest} :

$$\begin{aligned} R_n &:= \frac{\|U_n - \theta_n^* V\|^2}{\|U_n\|^2} \\ &= 1 - (\theta_n^*)^2 \frac{\|V\|^2}{\|U_n\|^2} \end{aligned} \quad (4.5)$$

It follows that $R_n \in [0, 1]$, with $R_n = 0$ if the signal power can fully be explained by the template part and $R_n = 1$ if the template can not explain for the signal power at all.

4.3 Academic Example

To support the theoretical framework in the previous part, we will show an academic example. We will use the template shown in Figure 4.2.

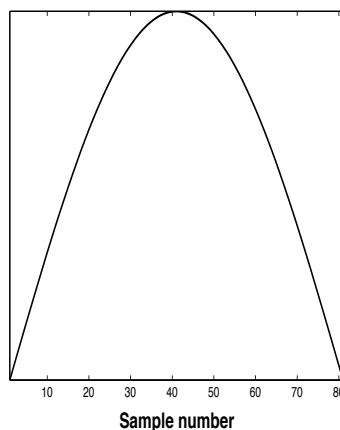
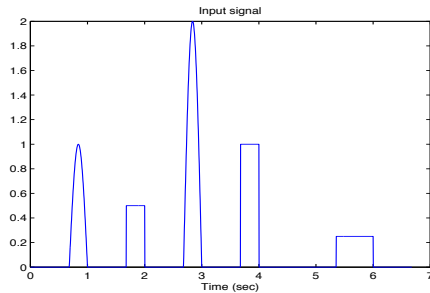


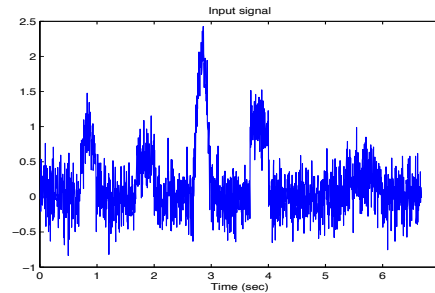
Figure 4.2: *Template for academic example of Section 4.3 ($M = 80$).*

Ideally, the signal being analysed is free of noise, i.e., only the epileptiform waveform pops up once in a while. In practice we also observe other transients, such as artifacts or events belonging to the EEG of sleep. Figure 4.3a shows a signal in which we want to detect the first and third events as scaled versions of the template (respectively with a factor one and two). The second, fourth and last transients are ‘non-epileptiform’. Figure 4.3c shows the output of the matched filter, θ_n^* . We see that θ_n^* peaks when the template has just passed and that the height of the peaks is proportional to the signals amplitude. Using only θ_n^* as feature for spike detection, however, also the other transients could be marked as events. That is exactly why we will add R_n as decision variable, shown in Figure 4.3e. Notice that $R_n = 1$ when we have the zero signal, and $R_n = 0$ when a (scaled version of a) spike is detected. θ_n^* and R_n together allow us to distinguish true spikes from other transients.

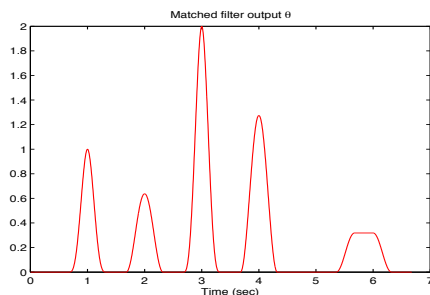
Figures 4.3b, 4.3d and 4.3f show the plots in case we add white noise to the signal. Again we see that the combination of θ_n^* and R_n allow for a successful distinction between spikes and other transients, although we need to find correct thresholds now.



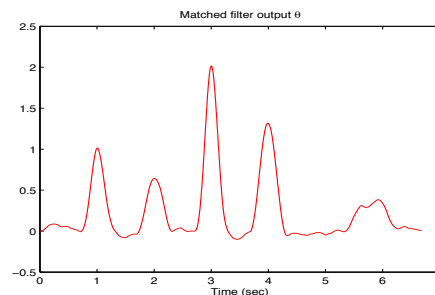
(a) *Input signal*



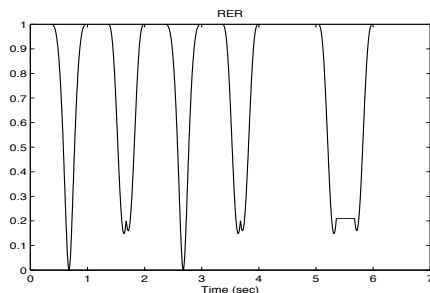
(b) *Input signal*



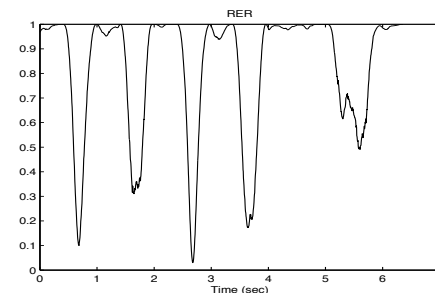
(c) *Output θ_n^* of the matched filter.*



(d) *Output θ_n^* of the matched filter.*



(e) R_n



(f) R_n

Figure 4.3: Comparison of θ_n^* and R_n for a noise-free signal (left) and the same signal with added white noise (on the right).

4.4 Summary

Matched filtering is used to detect the presence of templates in signals contaminated by noise and can for example be used in spike detection in EEG. The output of the matched filter can be interpreted as a linear correlation coefficient.

The academic example of Section 4.3 supports our decision to add the *Ratio of Powers* (R_n) (Definition (4.5)) as decision variable. Figure 4.3 clearly shows that a decision based on the two variables θ_n^* and R_n allows for a better distinction between, for example, true epileptiform events and artifacts. That is more than desirable since this is one of the big challenges in spike detection.

The derivations of $\mathbb{E}(\theta_n^*)$, $\text{var}(\theta_n^*)$ and $\mathbb{E}(P_n^{\text{rest}})$ (see derivations (4.2), 4.3) and (4.4) show the influence of the noise in the signal and the power and size of the template on the performance of the filter. Most important conclusion is that the number of samples should be large enough to deal with the negative influence of the noise.

Chapter 5 explains in more detail how the matched filter can be used to detect epileptiform events. In this chapter we also find the results of matched filtering in spike detection.

Matched Filtering in Practice

This chapter explains more specific how matched filtering, discussed in Chapter 4, is used to detect interictal epileptiform discharges in EEG. Section 5.1 discusses how the matched filter is applied. Section 5.2 shows the results we have obtained applying the method on 10 EEG recordings. The chapter finishes with Section 5.3, which shows the preliminary results when using a library of templates. Using such a library might be the approach to take for the automation of spike detection in EEG.

5.1 Implementation

Figure 5.1 (page 36) shows the main process of our algorithm, from the EEG recording being given as input up to the candidate epileptiform discharges that are returned as output. The first step of the algorithm is the preprocessing of the the EEG recording. We then apply the matched filter, resulting in θ^* and R , the arrays constaining all θ_n^* and R_n . After thresholding on these parameters, the candidate spikes follow. Sections 5.1.1 to `refsection:thresholding` discuss these steps in more detail.

5.1.1 EEG Recordings

The EEG recordings provided for testing contain information on the electrodes used, the voltages measured at these electrodes, the sample rate (in our case all files were sampled at a rate of 250 Hz), the length of the record, the annotations and many others. *Annotations* are notes in the EEG file made by an electroencephalographer during analysis of a file and are for example added when a spike or eyeblink is detected. The annotations are essential in the evaluation of the performance of the algorithm.

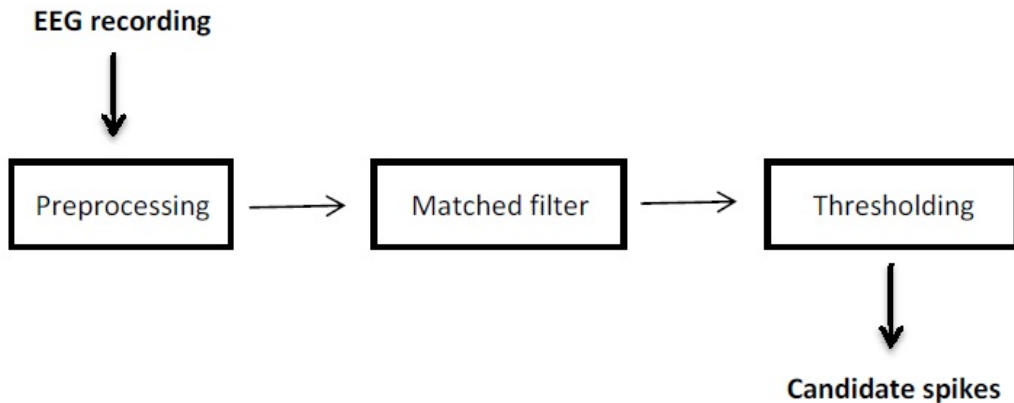


Figure 5.1: Block diagram showing the main process of matched filter to detect interictal epileptiform discharges.

5.1.2 Preprocessing

In the preprocessing step, the EEG-file is band passed filtered, eyeblinks are removed (both explained in Section 2.4) and a montage is chosen. In the study we used the $[4 - 20]$ Hz band for the bandpass filter and opted for the referential montage. The channels that are used in the analysis are the 19 channels $Fp1$, $Fp2$, $F3$, $F4$, $C3$, $C4$, $P3$, $P4$, $F7$, $F8$, $T3$, $T4$, $T5$, $T6$, $O1$, $O2$, Fz , Cz and Pz . In the preprocessing step we also choose the template to be used. This is done per file, after visual inspection of the spikes in the EEG-file (using the annotations). The epileptiform event that we consider the best representative of all the epileptiform discharges in the file is chosen as template.

5.1.3 Matched Filter

Using the referential montage, we obtain $U \in \mathbb{R}^{19 \times N}$, with N the number of samples per channel, that serves as input for the matched filter. The matched filter is fixed by our choice for the template $V \in \mathbb{R}^{1 \times (M+1)}$ and allows us to determine $\theta^* \in \mathbb{R}^{19 \times N}$ (Equation (4.1)). U , V and θ^* together allow to determine $R \in \mathbb{R}^{19 \times N}$ (Equation (5.2)).

5.1.4 Thresholding

Now that all θ_n^* and R_n have been calculated, we have to determine if candidate spikes have been found. To this end we will set the thresholds T_θ and T_R and a candidate

spike is found at time n if in at least one of the 19 channels

$$T_\theta \leq \theta_n \leq \frac{1}{T_\theta} \quad \text{and} \quad (5.1)$$

$$R_n \leq T_R \quad (5.2)$$

with $T_\theta, T_R \in [0, 1]$.

In the study we required a candidate spike to explain for at least 75% of the signal power and by that fixed T_R to 0.25, a somewhat arbitrary choice. We can justify this choice, however, by the fact that $T_R = 0.25$ demands a significant part of the signal power is being explained. Moreover it builds in some freedom which the results of Section refsection:academicexample show to be desirable.

The output of the method is an array, containing the times at which both the requirements (5.1) and (5.2) hold, i.e. an array containing all the times at which a candidate spike is found. In the case that candidate spikes are found within a range of 0.25 s of each other we assume them to correspond to the same EEG event. Such events are therefore clustered into a single event and instead of storing all individual time instances n , we store the mean time.

5.2 Results

In this section the results using matched filtering, as described in Section 5.1, are given. We will use the *Sensitivity* and *False Positives per Minute (FPM)* (Definitions (2.1) and (2.2)) as performance measures, where we count a candidate spike as *True Positive* if the event lies within a range of one second of an annotated spike, and as *False Positive* otherwise.

We tested the approach on 10 different EEG files and used the ROC-curve to find the ‘optimal’ threshold T_θ per file. The theoretical optimum is reached when we have a sensitivity of 1 and an *FPM* of 0, i.e., when we are in the upper left corner. This point is not always in reach of an algorithm and it is a natural choice to define the point on the curve closest to the corner as optimal. We call the minimal distance from this point to the corner. Since we think it is more rewarding to find an extra spike than it is inconvenient to find an extra false positive event, we will use a slightly different definition of α , somewhat arbitrarily set to

$$\alpha := \sqrt{(1 - \text{sensitivity})^2 + \frac{FPM^2}{2}} \quad (5.3)$$

The sensitivities and FPMs summarized in Table 5.1 are the values corresponding to that T_θ minimizing α . In this table we find the name of the file being analysed, the length of the file, the number of annotated spikes, the ‘optimal’ T_θ and of course the sensitivity and FPM.

The templates with which these results are obtained can be found in Appendix . We see that we can distinguish 3 types of templates; the spike and slow wave complex

of file a0009672, the group of sinusoid templates and the group of halve sines. In all tests we used the template as shown, except in the case of file b0006701 where the template was scaled by a factor 1.5.

In Table 5.2 some extra results are given. It shows that, as assumed, the morphology of eyeblink artifacts is quite similar to that of epileptiform discharges as removing them results in an improved α . It also shows that some of the templates are quite alike. $T_R = 0.25$ shows not to be optimal in all cases, as can be seen for file a0009369. Setting T_R to 0.1, the sensitivity of 1 remains, but we find a *FPM* of 0.2002. We also see that if we take $T_\theta = 0.375$ for file a0009672, the sensitivity increases to 0.9563. If we use these two results instead of the ones in Table 5.1, the total sensitivity increases to 95.12% with a *FPM* of 0.2113.

Figure 5.2 shows the ROC curve for the three different T_R settings used for the detection of candidate spikes in file a0009672. It shows that the curve corresponding to $T_R = 0.25$ lies ‘closest’ to the upper left corner, implying this threshold setting to result in the smallest α .

Filename	Length (min)	Nr. spikes	T_θ	Sensitivity	FPM
a0006732	16:20	11	0.8	1	0
a0006735	22:30	10	0.85	0.9	0.2224
a0007223	20:00	5	0.95	1	0
a0009369	20:00	3	0.45	1	0.5505
a0009672	19:50	206	0.6	0.835	0.2019
a0010617	20:00	8	0.9	1	0.05
b0005801	20:00	14	0.6	0.9286	0
b0006701	20:00	10	0.8	0.8	0.2467
b0007441	21:00	14	0.65	0.9286	0.0477
o0002133	20:00	6	0.7	1	0
Total:	179:40	287	-	0.8641	0.1503

Table 5.1: Detection results for 10 EEG files using the matched filter algorithm with a single file-specific template per file and fixed T_R .

Filename	T_R	T_θ	Sensitivity	FPM	Remark
a0006732	0.25	0.8	1	0	
	0.25	0.8	1	3.4934	eyeblinks not removed
a0009369	0.25	0.45	1	0.5505	
	0.1	0.45	1	0.2002	$< T_R$
	1	0.45	1	1.0509	$> T_R$
a0009672	0.25	0.6	0.8350	0.2019	
	0.25	0.375	0.9563	1.1102	$< T_\theta$
	0.1	0.6	0.6553	0.0505	$< T_R$
	1	0.6	0.8495	0.4037	$> T_R$
	0.25	0.95	0.8350	2.4727	using template b0007441
a0010617	0.25	0.9	1	0.05	
	0.25	0.8	1	0.05	using template b0007441
b0007441	0.25	0.65	0.9286	0.0477	
	0.25	0.5	0.8571	0.143	using template a0010617

Table 5.2: Some additive results on the results given in Table 5.1. In all cases we give the original results with fixed T_R and ‘optimal’ T_θ . Then some additive results are given in case one variable, the input U , one of the thresholds or the template V , has changed. In case a different template is chosen the thresholds correspond to the setting that minimizes the (adapted) α (Definition (5.3)).

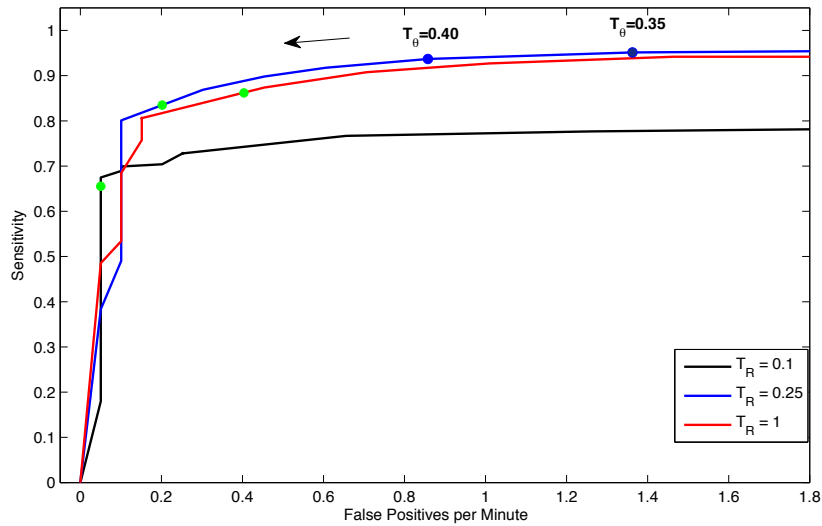


Figure 5.2: ROC-curves obtained using $T_R = \{0.1, 0.25, 1\}$. The green markers represent the optimal points.

5.3 Library of Templates

The ultimate goal in this area of research is to completely automate the detection of (candidate) spikes in EEG. Therefore we need a different approach than the method showed using file-specific templates. We need a general approach, capable of analysing arbitrary EEG recordings. An idea for such an approach is to form a library of templates that together cover all spike events that are known to occur. Running all templates over the file, it has to be decided if events found are of an epileptic kind or not. The fact that in a single EEG recording it is not uncommon that the epileptic discharges shown can be classified into more than one group, if classified on their morphology [26], supports the choice of working with a library.

To get an idea of the performance of such an approach, a library is formed, containing 9 of the 10 templates that were obtained previously. The template of file b0006701 is left out as its amplitude is significantly smaller than the other ones and is assumed to result in many false positives. For each template, T_θ is chosen as the value in Table 5.1) with $T_R = 0.25$. We say a (candidate) spike is found if two or more templates indicate an epileptiform event is found, which is an arbitrary choice.

We used two files, not used before, to test the algorithm of matched filtering with a library of templates. For file a0007908, 21:40 minutes long and containing 23 epileptiform events, this resulted in a sensitivity of 78.26% and 0.2309 false positives per minute. For file a0008921, 22:30 minutes long and containing 75 epileptiform events, a sensitivity of 82.67% was found with 2.8021 false positives per minute. The high FPM in the last is, at least partially, explained by the fact that the EEG record was not free of eyeblink artifacts (the eyeblink filtering failed).

This research aimed to make a first step towards the automated detection of interictal epileptiform discharges in EEG. We wanted to develop a method that will support encephalographers in the visual analysis of EEG recordings by detecting candidate epileptiform discharges.

Indiradevi et al. [11] obtained a sensitivity of 91.2% using wavelet analysis to detect epileptic spikes. Preliminary results obtained after implementing their approach show wavelet analysis to be quite powerful in detecting spikes. The fact that the choice for a template is not free and the non-intuitive threshold made us propose a different method.

This method is based on the theory of matched filtering. Candidate spikes are detected if the match of a chosen template with the EEG signal is significant. Moreover the template has to be able to explain for a significant part of the signal power. In our approach file-specific templates are used, with a fixed power threshold of 75%. Optimizing the corresponding correlation coefficient results in a *sensitivity* of 86.41% with 0.1503 *False Positives per Minute (FPM)*. This is a lower bound for our data set (containing 10 EEG recordings), as we have shown a sensitivity of 95.12%, with a FPM of 0.2122, can be obtained as well.

This method, however, is not a time-reducing approach. A suitable template has to be selected, requiring the entire file to be scanned in advance. We propose the use of matched filtering with a library of templates as approach for automated spike detection. Preliminary results were obtained on two new EEG recordings. A library of just 9 templates and fairly simple rules that define an event as epileptiform or not, were used. The results are promising as we obtained sensitivities of around 80%, with few false positives per minute.

Discussion and Recommendations

The proposed method uses the matched filter, the optimal filter maximizing the signal-to-noise ratio in the presence of additive noise. The EEG signal, however, is a very complex signal. Up to now, no proper model has been found to explain for it. The results in this study show that modelling the EEG signal as the superposition of spike behaviour and additive white noise works, as a sensitivity of above 95% can be obtained with just 0.2122 false positives per minute. This might be explained by the fact that epileptiform discharges are assumed to be individual events, interrupting the ongoing activity and not being influenced by it [26].

The choice of α as optimal point on the ROC curve is an important point of discussion. One encephalographer might prefer as few false positives as possible, where another EEG-er might want all true spikes to be found even if this is at the expense of more false positives. A proper definition of ‘optimal’ does not exist. We saw that for file a0009672 a sensitivity of 83.50% could be found with 0.1503 false positives per minute. It might however be preferred to obtain a sensitivity of 95.63% with 0.2113 false positives per minute, implying that α should be defined differently.

In this study a fixed T_R was used, with T_θ set such that α is optimized. Optimizing α for the combination of T_R and T_θ would probably result in even better, or at least, similar results. This, however, is computationally hard and the results obtained are thought to be convincing enough to support the choice for matched filtering. The same remarks can be made in regard of the somewhat arbitrary choice for templates.

The results of Table 5.2 show the big influence threshold settings have. For file a0009369, decreasing T_R decreases the FPM as well, at the same time holding on to a sensitivity of 1. The same effects are partly seen in case of file a0009672. Decreasing T_R results in a decreased FPM as well, but also in a decreased sensitivity. An explanation might be found in the fact that the (background) activity in two recordings can differ significantly. It might therefore be an idea to take, for example,

the standard deviation of the signal into account when threshold settings are chosen. The template of file b0006701, with its significantly smaller amplitude in comparison to the other 9 templates used, also advocates for such a consideration.

Our approach, with the file-specific templates, differs on several points with the approach of electroencephalographers when analysing an EEG record. The first difference is that electroencephalographers take the spatial distribution of an EEG event into account; in which channels is an event found? This information is used to distinguish epileptiform events from artifacts. In case of an epileptiform event, this information is also used to localize the epileptic foci and by that classifying the type of epilepsy shown. In our approach, a candidate spike is detected if the thresholds T_θ and T_R are exceeded in one of the EEG channels. Which channel this is does not matter. Electroencephalographers also take the physical state of the patient into account, which is not implemented in our approach. If the patient has his eyes open or shut, is asleep or is possibly in a state of hyperventilation (this technique is used to provoke epileptiform discharges), this can be found in the annotations. An electroencephalographer can thereby ascribe events to an expected cause (sleep for example) instead of to an epileptiform cause. At last electroencephalographers can use several montages to ensure themselves they have found an epileptiform event when in doubt, whereas our approach only works on the referential montage. All the above points could be taken into account in the development of a spike detection programme, as to support electroencephalographers the best as possible.

Matched filtering with file-specific templates (sensitivity of 95.12%, FPM of 0.2122) outperforms the many methods reviewed by Halford [10]. These methods, however, were developed for the goal of automated spike detection. Using a library of 9 templates, with fairly simple rules defining an event as epileptiform or not, showed to be promising for automated spike detection as well. To truly outperform the previous methods though, some important issues have to be dealt with. The first is setting up a library that contains templates covering all of the epileptiform events known. Most important is the question which rules are required to truly be able to distinguish epileptiform discharges from other EEG activity.

Acknowledgements

This master thesis would not have come to an end without Michel van Putten and Shaun Lodder, of the chair Clinical Neurophysiology (department Technical Medicine). They gave me the oppurtonity to work on this project, which was performed as part of Shauns Ph.D. research. It gave me the opportunity to work an a truely *applied* mathematical subject. It was nice working with you guys, you made me feel more than welcome to come by for support, questions and to discuss new ideas or obtained results.

Most of my gratitude goes out to Gjerrit Meinsma, who was my daily supervisor during the project. Thanks fory your help and ideas during the project, the support, the talks that helped me through some tough days, but most of all for your infinite enthusiasm. It was a pleasure working with you.

A ‘thank you’ is also reserved for my fellow students. Thanks for attending all the lectures with me and for working together on projects, excercises and towards exams. It made studying more pleasant. And off course I will never forget the numerous lunch breaks spend on playing cards.

My dear friends, in Enschede, but also outside: thanks for all the pleasant dinners, evenings and trips and for just being there if things did not go as planned. You made me feel loved and enjoy life to the fullest.

Last, but certainly not least, I want to thank my family. Most of the time they had no idea how my life looked like being a mathematics student (and who can blaim them), but they were proud of me anyhow. I especially want to thank my parents for supporting me, not only now, but throughout my life. In good times, or bad, I can always discuss my life, thoughts and problems with you. Thanks for being the warm and save place I know I can always return home to.

Templates

This appendix shows the templates used to obtain the results of Table 5.1 (using $T_R = 0.25$ and T_θ such that α is optimized). The figures shows part of the signal the template originates from, and the actual template that was used. Based on the morphologies, the templates can be classified into three groups; the spike-wave complex of Figure 1, the half sines of Figures 2 to 6 and the sines of Figures 7 to 10.

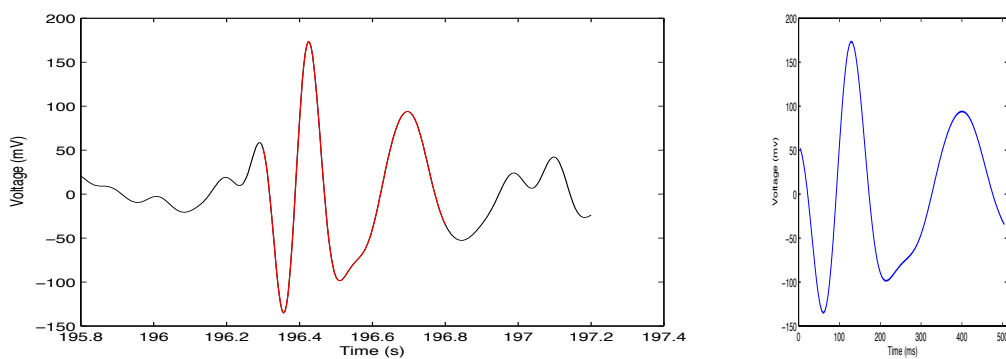


Figure 1: *Template - file a0009672.*

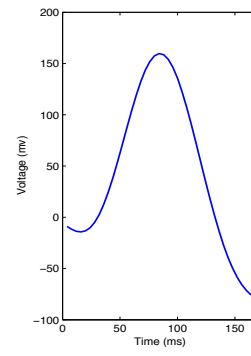
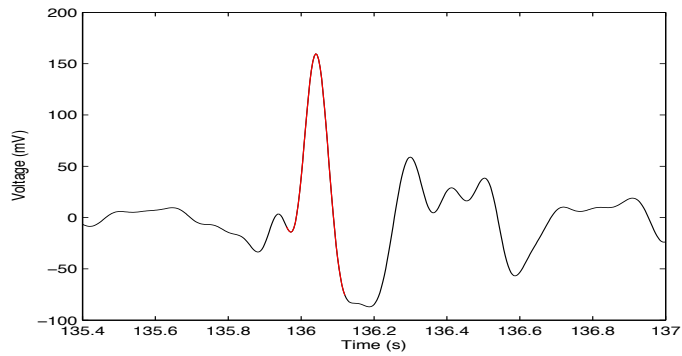


Figure 2: *Template - file a0006732.*

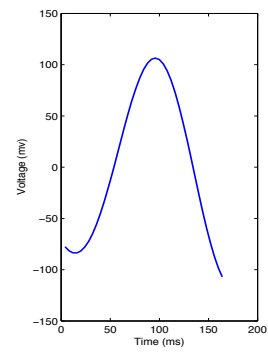
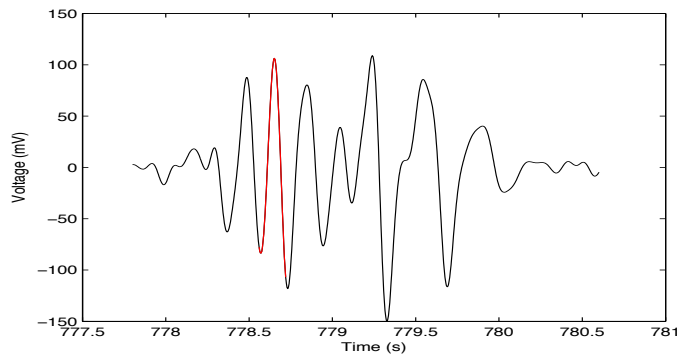


Figure 3: *Template - file a0007223.*

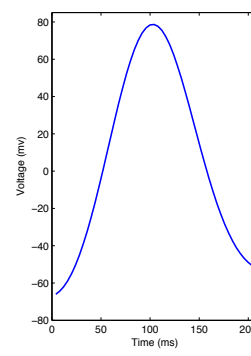
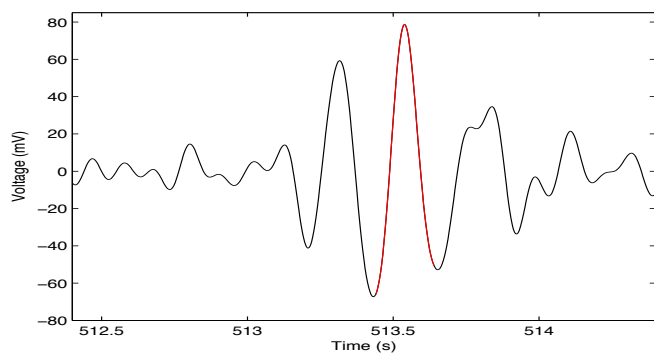


Figure 4: *Template - file a0010617.*

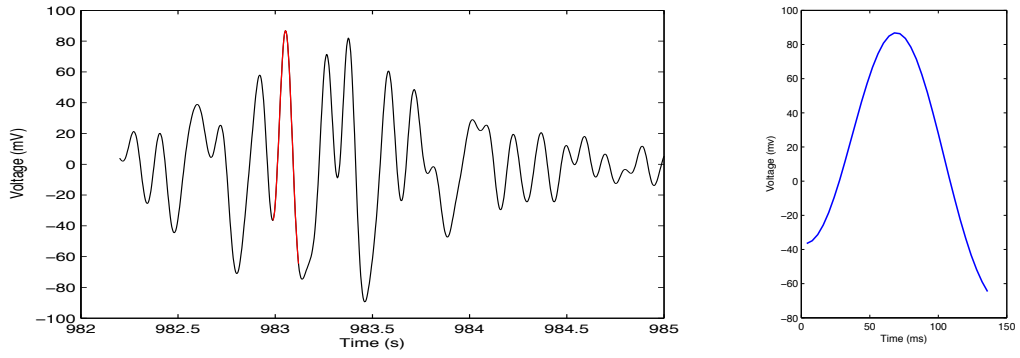


Figure 5: *Template - file b0005801.*

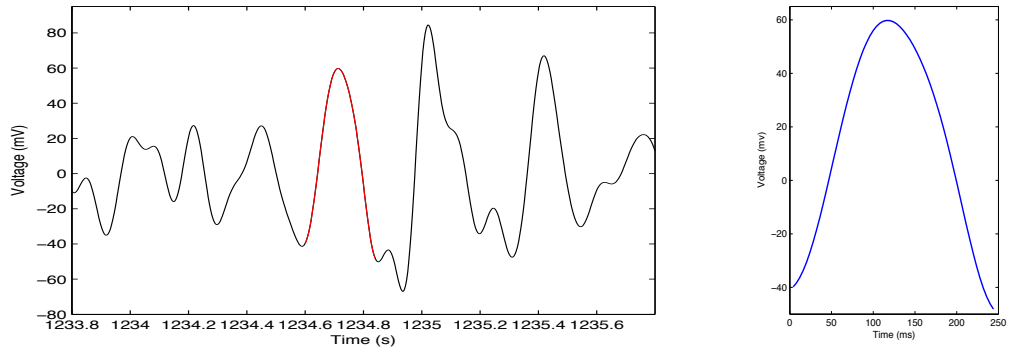


Figure 6: *Template - file o0002133.*

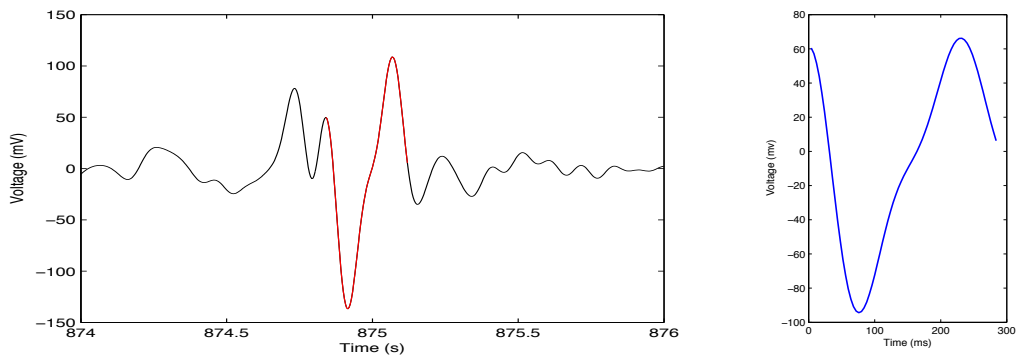


Figure 7: *Template - file a0006735.*

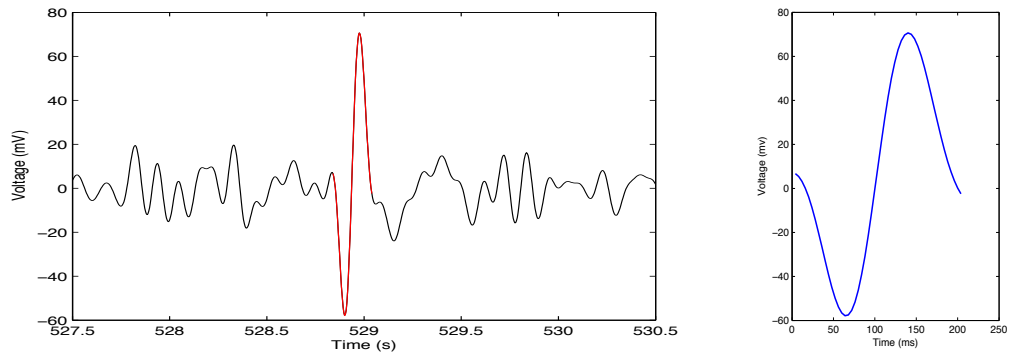


Figure 8: *Template - file a0009369.*

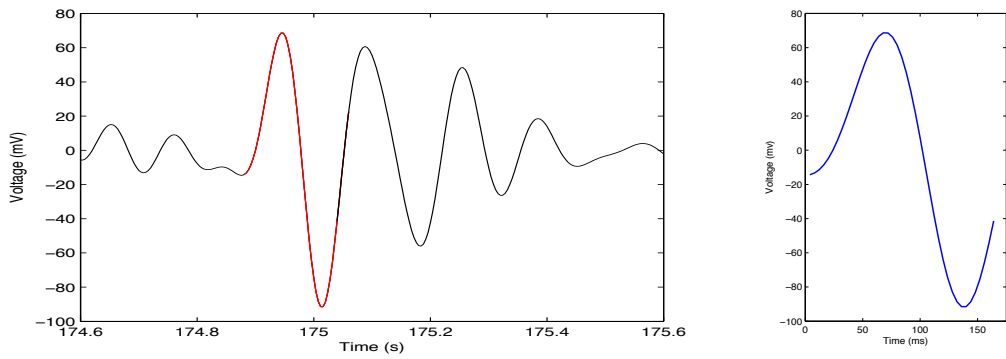


Figure 9: *Template - file b0006701.*

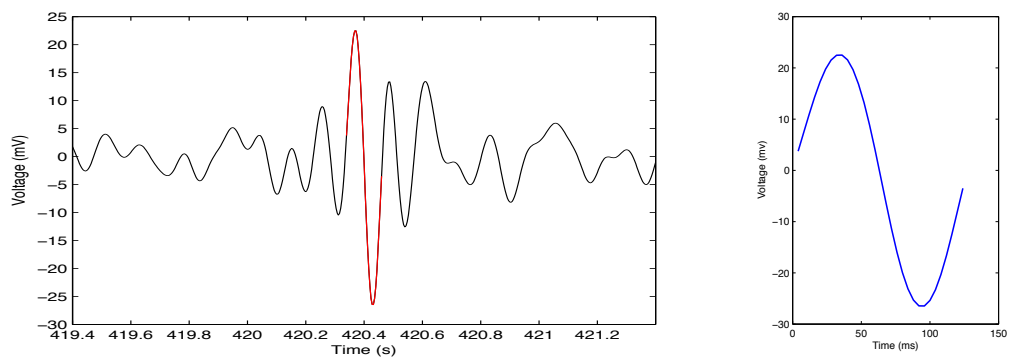


Figure 10: *Template - file b0007441.*

In this appendix we find the two main scripts used in this study. The first is Matlab script *matchfilter.m* in which matched filtering is applied to detect the epileptiform discharges in a given signal. The output of this script was evaluated using the script *quality.m*. At last we added the file *wavelet.m*, which was used to produce the figures of the implementation of Indiradevi et al [11].

```
function [IEDs] = matchfilter(file,template,T,R)

% matchfilter - uses matched filtering to find specified events
%               (in this case epileptiform discharges)
%
% Syntax:  [IEDs] = matchfilter(file,template,T,R)
%
% Inputs:
%   file      - preprocessed EEG-file (.mat)
%   template  - template of an epileptiform discharge
%   T         - threshold for theta (in [0,1])
%   R         - threshold for R.n (in [0,1])
%
% Output:
%   IEDS     - array with times were candidate spikes are found
%
%-----Begin code-----

u = file; u2 = u.^2;
N = length(u); fs = 250;

%% Spike-template
V = flipud(template);
M = length(V); normV = norm(V)^2;
g = (V'*V)\V';

%% Matched filter
```

```

tg = filter(g,1,u); tg = abs(tg);
tg2 = tg.^2;

%% Power template part
PowerT = normV .* filter(ones(1,1),M+1,tg2);

%% Thresholding
detected = zeros(N,2);
PowerU = [];

for i = 1:19

    PowerU = filter(ones(1,M+1),M+1,u2(:,i));
    PRest = PowerU - PowerT(:,i);
    RatioP(:,i) = PRest./PowerU;

    for j = 1:length(RatioP)
        if RatioP(j,i) ≤ R && tg(j,i) ≥ T && tg(j,i) ≤ 1/T
            detected(j,1) = detected(j,1) + 1;
        end
    end
end

%% Array with hits and # of consecutive hits
IEDs = [0 0]; k = 0;
for i = 2:N
    if detected(i,1) ≠ detected(i-1,1)
        if detected(i,1) == 1; %new hit
            k = k + 1;
            IEDs(k,1) = i;
        end
    else
        if detected(i,1) == 1; %consecutive hit
            IEDs(k,2) = IEDs(k,2) + 1;
        end
    end
end

%% Determining times of hits in (s)
for i = 1:k
    if IEDs(i,2) ≠ 0
        IEDs(i,1) = IEDs(i,1)/fs + mean(1:IEDs(i,2))/fs ...
            - size(template,1)/fs;
    else
        IEDs(i,1) = (IEDs(i,1)/fs - size(template,1))/fs;
    end
end

%% No IEDs found?
if IEDs(1,1) == [0 0];
    disp('No IEDs found!')
    IEDs = [];
end

```

```

    return
end

%% Joining hits corresponding to the same event
gr = length(IEDs(:,1));
equals = zeros(gr,1);
if gr > 1
    for i = 1:gr-1
        if IEDs(i+1,1)-IEDs(i,1) < 0.25
            equals(i) = 1;
        end
    end
end

for i = 1:length(equals)
    if equals(i) == 1
        IEDs(i,1) = 0;
    end
end

%% Ouput
IEDs = unique(IEDs(:,1));
if IEDs(1,1) == 0
    IEDs = IEDs(2:end,1);
end

end

```

```

function [sensitivity FPM] = quality(IEDs,pgs,N)
% function IEDs_missed = quality(IEDs,pgs,N)
% function IEDs_false = quality(IEDs,pgs,N)
%
%
% Input:    - IEDs: array of times (s) were spikes are found
%           - pgs: array with times (s) of annotated spikes
%           - N: length of signal (number of samples)
%
% Outputs:  (i)    sensitivity and FPM
%           (ii)   array with times of false negatives
%           (iii)  array with times of false positives
%
%-----Begin code-----
nr_correct = 0;
indexes_correct = []; indexes_false = [];
IEDs_missed = pgs; IEDs_correct = []; IEDs_false = [];

fs = 250;
k = size(IEDs,1);
n = length(pgs);

```

```

%% FP's and FN's
% Loop through all hits to see if it matches an annotation,
% hit within one second of annotation: True Positive.
for i = 1:k
    start = 1; k = 0;
    for j = start:n
        m = abs( IEDs(i,1) - ...
            [pgs(j,1) : 0.025 : pgs(j,1)+pgs(j,2)] );
        if min(m) < 1
            nr_correct = nr_correct + 1;
            indexes_correct = cat(2,indexes_correct,j);
            start = j;
            k = 1;
        end
    end
    if k == 0
        indexes_false = cat(2,indexes_false,i);
    end
end

indexes_correct = unique( sort(indexes_correct,'ascend') );
for i = indexes_correct(1:end)
    IEDs_missed(i) = 0;
    IEDs_correct = cat(2,IEDs_correct,pgs(i));
end

IEDs_missed = sort(unique(IEDs_missed(:,1)));
if IEDs_missed(1) == 0;
    IEDs_missed = IEDs_missed(2:end);
end

for i = indexes_false
    IEDs_false = cat(2,IEDs_false,IEDs(i));
end

%% Sensitivity and FPM
sensitivity = length(unique(IEDs_correct)) / length(pgs);
FPM = (length(IEDs_false) / N) * (250*60);

end

```

```

function wavelet(seg,pgs)

% detectIED - performs a discrete wavelet transform (Db4) on
% the input signal and determines if the value of the
% squares of reconstructed wavelet coefficients at
% levels 4 and 5 exceed a threshold.
% If the threshold is exceeded, an IED is detected.
% [ Inspired by Indiradevi et al. (2008).]
%

```

```

% Syntax: [IEDs] = wavelet(seg,pgs,stdev)
%
% Inputs:  - seg: signal in .mat-extension
%          - pgs: array with times (s) of annotated spikes
%
% Output:  - plot of squared reconstructed detail coefficients,
%           corresponding thresholds and annotated spikes
%
%
%-----Begin code-----
N = length(seg);
fs = 250;

% Standard deviation of 19 channels used
stdev = std(seg); stdev = mean(stdev);

% Wavelet decomposition
[C,L] = wavedec(seg(:,3),6,'db4'); % select one channel

% Extracting detail coefficients at all scales
[D4,D5] = detcoef(C,L,[4 5]);

% Reconstruct detail coefficients
Y4 = upcoef('d',D4,'db4',4,N); Y5 = upcoef('d',D5,'db4',5,N);

% Plot signal, squared detail coefficients and thresholds
grwav = 2.2580;
gw4 = grwav/4; gw5 = grwav/(4*sqrt(2));

t = 0: (1/250) : (N-1)/250;
t4 = 0: (1/250)*16 : (N-1)/250;
t5 = 0: (1/250)*32 : (N-1)/250;

figure()
subplot(2,1,1)
plot(t4,D4(4:18503).*D4(4:18503),'k'); hold on
for i = 1:size(pgs)
    for k = pgs(i,1):0.025:pgs(i,1)+pgs(i,2)
        plot(k,1*10^5,'g. '); hold on
    end
end
plot( (1:length(Y4))/250, (stdev/gw4) * abs(Y4) * 2^4 , 'r' )
title('Scale 4')

subplot(2,1,2)
plot(t5,D5(4:9253).*D5(4:9253),'k'); hold on
for i = 1:size(pgs)
    for k = pgs(i,1):0.025:pgs(i,1)+pgs(i,2)
        plot(k,5*10^5,'g. '); hold on
    end
end
plot( (1:length(Y5))/250, (stdev/gw5) * abs(Y5) * 2^5 , 'r' )

```

```
title('Scale 5')  
end
```

Bibliography

- [1] J. ASKAMP. Personal communication, 2012.
- [2] R. BARANIUK, *Matched filter*. <http://cnx.org/content/m34685/latest/>. Accessed: June 2012.
- [3] S. R. BENBADIS AND D. RIELO, *Eeg artifacts*. <http://emedicine.medscape.com/article/1140247-overview#showall>. Accessed: April 2012.
- [4] C. D. BROWN AND H. T. DAVIS, *Receiver operating characteristics curves and related decision measures: a tutorial*, Chemometrics and Intelligent Laboratory Systems, 80 (2006), pp. 25–38.
- [5] H. G. ET AL, *Wavelet analysis of transient biomedical signals and its application to detection of epileptiform activity in the eeg*, Clinical Electroencephalography, 31 (4) (2000), pp. 181–191.
- [6] G. FISCHER, N. MARS, AND F. LOPEZ DA SILVA, *Pattern recognition of epileptiform transients in the electroencephalogram*, Tech. Report 7, Institute of Medical Physics, Da Costakade, Utrecht, Netherlands, 1980.
- [7] P. GLOOR, *Contributions of electroencephalography and electrocorticography to the neurosurgical treatment of the epilepsies*, Advances in Neurology, 8 (1975), pp. 59–105.
- [8] A. GRAPS, *Wavelet vs fourier transforms*. http://www.amara.com/IEEEwave/IW_wave_vs_four.html. Accessed: May 2012.
- [9] —, *An introduction to wavelets*, IEEE Computational Science and Engineering, 2 (1995).
- [10] J. J. HALFORD, *Computerized epileptiform transienst detection in the scalp electroencephalogram: Obstacels to progress and the example of computerized eeg interpretation*, Clinical Neurophysiology, 120 (2009), pp. 1909–1915.

- [11] K. INDIRADEVI ET AL, *A multi-level wavelet approach for automatic detection of epileptic spikes in the electroencephalogram*, Computers in Biology and Medicine, 38 (2008), pp. 805–816.
- [12] J. JACKSON, *On the anatomical, physiological, and pathological investigation of epilepsies*, (1913).
- [13] T. KALAYCI AND O. OZDAMAR, *Wavelet preprocessing for automated neural network detection of eeg spikes*, Engineering in Medicine and Biology Magazine - IEEE, 14 (1995), pp. 160–166.
- [14] M. LATKA, Z. WAS, A. KOZIK, AND B. J. WEST, *Wavelet analysis of epileptic spikes*, Physical Review E, 67 (2003).
- [15] M. H. LIBENSON, *Practical Approach to Electroencephalography*, Saunders, Philadelphia, first ed., 2009.
- [16] S. S. LODDER. Personal communication, 2012.
- [17] T. LOSEY AND L. UBER-ZAK, *Time to first interictal discharge in extended recording eegs*, Clinical Neurophysiology, 25 (2008), pp. 357–360.
- [18] P. MODUR AND B. RIGDON, *Diagnostic yield of sequential routine eeg and extended outpatient video-eeg monitoring*, Clinical Neurophysiology, 119 (2008), pp. 190–196.
- [19] C. MOYES AND M. JIANG. http://people.ece.cornell.edu/land/courses/ece4760/FinalProjects/s2012/cwm55/cwm55_mj294/index.html.
- [20] I. F. OF SOCIETIES FOR CLINICAL NEUROPHYSIOLOGY, *A glossary of terms most commonly used by clinical encephalographers*, Electroencephalographic Clinical Neurophysiology, 37 (1974), pp. 538–548.
- [21] PSYCHOLOGY-WIKI, *K-complex*. <http://psychology.wikia.com/wiki/K-complex>. Accessed: July 2012.
- [22] F. SARTORETTO AND M. ERMANI, *Automatic detection of epileptiform activity by single-level wavelet analysis*, Clinical Neurophysiology, 110 (1999), pp. 239–49.
- [23] L. SENHADJI, J.-L. DILLENSEGER, F. WENDLING, C. ROCHA, AND A. KINIE, *Wavelet analysis of eeg for three-dimensional mapping of epileptic events*, Annals of Biomedical Engineering, 23 (1995), pp. 543–552.
- [24] J. R. STEVENS, B. L. LONSBURY, AND S. L. GOEL, *Seizure occurrence and interspike interval - telemetered electroencephalogram studies*, Archives of Neurology, 26 (1972), pp. 409–419.

- [25] C. VAN DONSELAAR, R. SCHIMSHEIMER, A. GEERTS, AND A. DECLERCK, *Value of the electroencephalography in adult patients with untreated idiopathic first seizures*, Archives of Neurology, 49 (1992), pp. 231–237.
- [26] M. J. VAN PUTTEN. Personal communication, 2012.
- [27] S. WILSON, R. HARNER, F. DUFFY, B. THARP, M. NUWER, AND M. SPERLING, *Spike detection. i. correlation and reliability of human experts*, Electroencephalography and Clinical Neurophysiology, 98 (1996), pp. 186–198.